Amino Acid Catabolism in *Fusobacterium nucleatum* and *Fusobacterium varium*

by

Felix S. Lee

*Submitted in Partial Fulfilment of the
Requirements for the Degree of Master of Science*

at

Dalhousie University
Halifax, Nova Scotia
August 28, 2000

0-612-57203-X

Canada

For My Family

Table of Contents

List of Figures

List of Tables

Abstract

The catabolism of the amino acids glutamate, histidine, and lysine was investigated in this study. Both the D- and L-isomers of the three amino acids were catabolized by F. nucleatum and F. varium resuspensions to acetate and butyrate, plus formate from hisitidine. All three of the D-amino acids were consumed slower than the L-isomers of the corresponding amino acids.

A pathway involving the conversion of acetate to butyrate contains the intermediates acetoacetyl-CoA, 3-hydroxybutyryl-CoA, and crotonyl-CoA. The acid forms of these three esters were utilized by the two Fusobacterium species, with a distinct preference for (S)-3-hydroxybutyrate over its (R)-isomer.

The formation of butyrate from the L-isomers of three amino acids was investigated using universally ^{13}C-labelled substrates to determine whether butyrate is derived directly from the amino acids as an intact C_4 unit or formed by the combination of two acetate-derived C_2 units. The former was established by the observation of a three-bond ^{13}C-^{13}C coupling in the ^{13}C-NMR spectrum of butyrate, isolated as a 4-bromophenacyl ester. In F. nucleatum, butyrate was formed as an intact C_4 unit from all three amino acids. On the other hand, only lysine produced an intact C_4 butyrate in F. varium. These results are consistent with the suggested pathways of amino acid degradation.

The catabolism of lysine by the two Fusobacterium species was investigated in greater detail to determine whether cleavage of the C_6 lysine molecule occurs between C-2 and C-3 or C-4 and C-5 to produce separate C_2 and C_4 units. Information in the literature suggests that separate catabolic pathways exist for each of the two isomers, and despite the lack of sufficient isotopic and enzymatic evidence, it is suggested that L-lysine is cleaved between C-2 and C-3, while D-lysine cleavage occurs between C-4 and C-5. Studies employing 2,3-^{13}C$_2$- and 4,5-^{13}C$_2$-labelled L-lysine have demonstrated that cleavage of L-lysine occurs between C-2 and C-3.

List of Abbreviations

AcetylNAC	*N,S*-diacetylcysteamine
ATP	adenosine 5'-triphosphate
CoA	coenzyme A
δ	chemical shift
EC	enzyme classification number
FDA	*N*,α-(5-fluoro-2,4-dinitrophenyl)-L-alaninamide
HPLC	high performance liquid chromatography
in vacuo	under reduced pressure
J	coupling constant
m	multiplet
MS	mass spectrometry
m/z	mass-to-charge ratio
NAC	*N*-acetylcysteamine
NAD^+	nicotinamide adenine dinucleotide
NADH	nicotinamide adenine dinucleotide reduced form
NMR	nuclear magnetic resonance
OD_{660}	optical density at 660 nm
PBS	phosphate buffered saline
s	singlet
t	triplet
TLC	thin layer chromatography
UV	ultraviolet
v/v	volume/volume

Acknowledgements

Believe it or not, this page of acknowledgements has proved to be the most difficult page in the thesis to write. Sure, it seems easy because there's no chemistry content, but this page required intensive thought, as the details provided here are recalled from memory, not from notes written in lab books or scribbled on lab benches or the excellent writing surfaces of Kimwipes and brown paper towels. It is perhaps for that reason that my supervisor required that experiments and details be written in lab books.

Speaking of which, first and foremost, the utmost acknowledgements are expressed to my supervisor, Dr. Rob White. Thank you for the support, encouragement, advice, and suggestions, and for simply being there to answer three-hour questions related to the research or otherwise. It has made the past two years a real pleasure.

There are also other members of the Dalhousie community to whom acknowledgements should also be addressed. For instance, the members of my supervisory committee, Drs. Steve Bearne, Song Lee, and Jim Pincock for their time, effort, and interest. Drs. Don Hooper and Mike Lumsden for NMR service and also for jokes and stories. Dr. Stu Grossert for mass spectra and smiles. Drs. Russ Boyd and Fran Cozens, for assistance. The people on fifth floor of the chemistry department, particularly Dr. Peter Wentzell in the office next door, for tolerating the stench associated with anaerobic bacteria. And of course, all of the chemistry graduate students.

Not to be forgotten are the important people on the non-academic side, such as friends and lab-mates, for continuous encouragement and compassion, be they in the region, the land of the grain elevator, over and across the home of the Maritime lobster, or otherwise. These include my family, Richard Sparling, Amanda Delaney, Shannon Smith, Brian Sithoo, Cormac Murphy, Ross Witherell, and Satyendra Satyanarayana. The list is getting lengthy, but I might as well continue and not leave out Brian, Nicole, Shervin, Jesper, Amy, Stasa, and anyone else I know that I haven't mentioned.

Finally, for financial support during my program, obliged acknowledgements are extended to the Natural Sciences and Engineering Research Council of Canada, the Izaak Walton Killam Memorial Trust Fund, Dalhousie University, and the Walter. C. Sumner Foundation. In addition, an external travel grant for a conference was also provided by the generosity of the Canadian Society of Microbiologists.

Chapter 1: Introduction

1.1   Introduction

It is believed that life on Earth originated in an oxygen-free reducing environment and that the oxygen present in the atmosphere today was an end-product of metabolism by anaerobic bacteria. These anaerobes were widespread several billion years ago,[1] but the accumulation of toxic oxygen has limited their current existence to environments containing reduced amounts of oxygen.

Unlike their aerobic counterparts, many anaerobic bacteria obtain their energy and carbon sources through the process of fermentation, where complete oxidation of the substrates does not occur. For example, yeasts under anaerobic conditions ferment carbohydrates to ethanol, while aerobes such as humans fully oxidize carbohydrates to carbon dioxide. Anaerobic fermentation is also of historical significance: in the mid-1900's, *Clostridium acetobutylicum* provided the primary commercial source of acetone by carbohydrate fermentation.[2]

However, the fermentative process in anaerobes is not limited to carbohydrates. Amino acids that are present as individual monomers or as a peptide polymer are also catabolized; amino acids and small peptides are major energy and carbon sources for some anaerobic bacteria, such as those of the genus *Fusobacterium*.[3,4,5,6,7] Common end-products of amino acid fermentation include ammonia, carbon dioxide, hydrogen, and various short-chained fatty acids, such as acetate and butyrate.[8]

The physiology of bacteria is different from that found in more advanced organisms such as humans. It is these physiological differences that allow antibiotics to destroy bacteria without causing significant harm to the human host, as antibiotics target only the unique bacterial physiology. The classical antibiotic penicillin, as an example, targets the biosynthesis of peptidoglycan,[9,10] an essential component of bacterial cell walls.

Penicillin and its natural or semi-synthetic derivatives belong to a category of antibiotics known as the β-lactams, all of which target peptidoglycan biosynthesis. When bacteria develop resistance to β-lactams, rendering them ineffective, another category of antibiotics that has a different metabolic target would be required for treatment. However, only a limited number of targets for antibiotic attack are known.[11] To address the problematic and recently widespread emergence of resistance, novel antibiotics must be developed. Yet, instead of developing new antibiotics that have the same targets as the existing ones, new targets must be found.[11]

A potential target for new antibiotics would be amino acid fermentation, as these metabolic pathways are different in anaerobic bacteria and humans. In light of the medical relevance and pathogenicity of the *Fusobacterium* species,[12] the objective of the current studies lies in establishing a deeper understanding of the catabolism of the amino acids in two *Fusobacterium* species, *F. nucleatum* and *F. varium*, with an emphasis on glutamate, histidine, and lysine.

1.2 Utilization of Amino Acids by Two *Fusobacterium* Species

Initial studies on amino acid usage by *Fusobacterium* species have concentrated primarily on different strains of *F. nucleatum*,[3,4,5,13,14,15,16] the *Fusobacterium* species most implicated in periodontal disease.[12] Four amino acids, glutamate, histidine, lysine, and serine, were shown to be the preferred amino acids for most strains of *F. nucleatum*. Other amino acids were metabolised by some strains, while most hydrophobic and aromatic acids were metabolised poorly. Similar utilization patterns were observed in studies involving *F. varium*.[17] In addition, clinical isolates of *Fusobacterium* species utilized fewer amino acids than the reference strains,[15] and their repeated subculturing increased their ability to utilize amino acids.[18]

However, the initial studies of amino acid utilization demonstrated a lack of attention to stereochemistry, as either racemic amino acid mixtures or amino acids of unspecified stereochemistry were used. Normally, D-amino acids are rare and are not degraded by most organisms, including humans. Organisms that degrade D-amino acids either degrade them via pathways separate from the L-amino acids or converte them to the corresponding L-isomers prior to degradation. A more recent study focussed on the stereochemistry of amino acid uptake by *F. nucleatum* and *F. varium*.[19] Both isomers of lysine were utilized by the two species, and while *F. varium* utilized both isomers of glutamate, only the L-isomer was used by *F. nucleatum*. On the other hand, *F. varium* utilized only

the L-isomer of histidine, and both histidine isomers were catabolized by *F. nucleatum*.

Unfortunately, that recent study[19] was performed in complex medium of undefined composition. Interferences and competition from other carbon sources, including other amino acids present in the medium, may have affected the uptake of the amino acids being studied. Studies using *Fusobacterium* resuspensions in buffered systems, with minimal interferences from other carbon sources, would be expected to provide briefer and more accurate results on the specificity of amino acid uptake.

1.3   Conversion of Acetate to Butyrate

A central metabolic pathway (Figure 1) involving the conversion of acetate to butyrate is present in many anaerobic bacteria,[20,21,22] including the *Fusobacterium* species. Catabolism of amino acids, such as glutamate, histidine, and lysine, produces intermediates that feed into this pathway. Five major enzymes catalyse the conversion of acetate to butyrate: butyryl-CoA:acetate CoA-transferase (Figure 1, Step A); acetyl-CoA:acetyl-CoA acetyltransferase (thiolase) (Figure 1, Step B); NAD^+-dependent 3-hydroxybutyryl-CoA dehydrogenase (Figure 1, Step C); crotonase (Figure 1, Step D); and NAD^+-dependent butyryl-CoA dehydrogenase (Figure 1, Step E). Activities of these enzymes have been detected and the enzymes have been studied in *F. nucleatum*[23] and other anaerobic species.[20,24,25] Isotopic evidence using

deuterium labelling has also identified the pathway in *F. nucleatum* and *F. varium*.[26,27] Acetyl-CoA from the pathway can also be converted to acetic acid in the production of ATP.
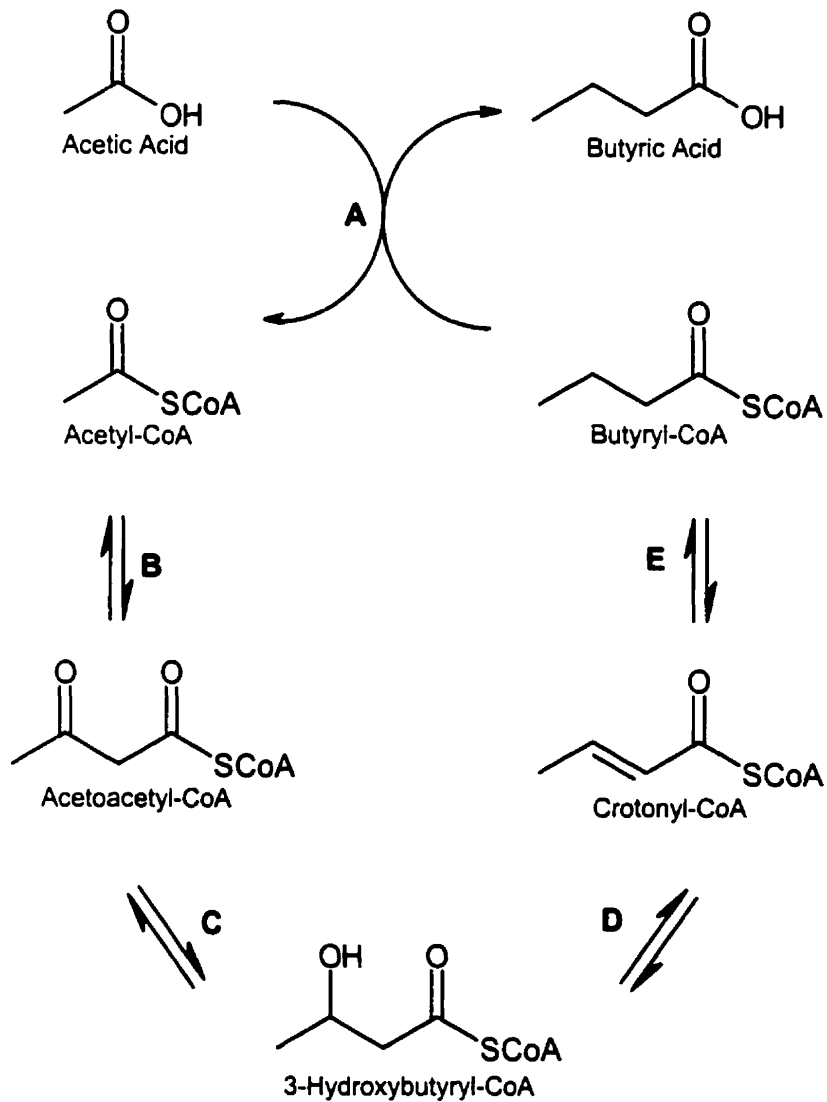
Figure 1. Conversion of acetate to butyrate: the central metabolic pathway in anaerobic bacteria. (A) Butyryl-CoA:acetate CoA-transferase (EC 2.8.3.8). (B) Acetyl-CoA:acetyl-CoA acetyltransferase (thiolase; EC 2.3.1.9). (C) Hydroxybutyryl-CoA dehydrogenase (EC 1.1.1.35). (D) Crotonase (EC 4.2.1.17). (E) Butyryl-CoA dehydrogenase (EC 1.3.99.2).

In anaerobic fermentation processes, where oxygen is not available as a terminal electron acceptor, other reducible substrates are used to regenerate NAD^+ from the NADH formed from the oxidative steps of amino acid catabolism. Whereas, in aerobic organisms, oxygen is available for the regeneration process, which also harnesses the reducing power of NADH to create ATP via the electron transport chain. In anaerobic organisms, no ATP is gained from the regeneration process. Hence, the only physiological significance of the acetate-butyrate pathway lies in the regeneration of NADH to NAD^+, where two NAD^+ are regenerated by the conversion of acetate to butyrate. Consequently, butyrate is assumed to be a dead-end metabolic end-product, even though the possible reverse conversion of butyrate to acetate has not been investigated by isotopic studies.

Interestingly, there have been no studies in anaerobic bacteria on the catabolism of the acid forms, not the CoA esters, of the three key intermediates in the acetate-butyrate pathway. The acid forms of these three intermediates, acetoacetate, 3-hydroxybutyrate, and crotonate would provide ATP when degraded to acetate and/or butyrate end-products. In other words, the ability of the organism to degrade these substrates is beneficial from an energetics standpoint.

Metabolism of acetoacetate, 3-hydroxybutyrate, and crotonate first requires their conversion to CoA esters, a process requiring the equivalent of one mole of ATP per mole of acid. As the CoA esters are intermediates in the acetate-butyrate pathway, entry into the pathway is possible. The ratio of end-products can be predicted by determining the ratio required to achieve no net production of NADH (Figure 2).

A Acetoacetate ⟶ Acetoacetyl-CoA ⟶ 2 Acetyl-CoA ⟶ 2 Acetate

ATP

Net: 1 ATP and 2 acetate per acetoacetate   2 ATP

B 2 3-Hydroxybutyrate ⟶ 2 3-Hydroxybutyryl-CoA

2 ATP   NADH

Acetoacetyl-CoA   Crotonyl-CoA

**Net: 1 ATP, 2 acetate, and
1 butyrate per 2 3-hydroxybutyrate**

NADH

2 Acetyl-CoA   Butyryl-CoA

2 ATP   ATP
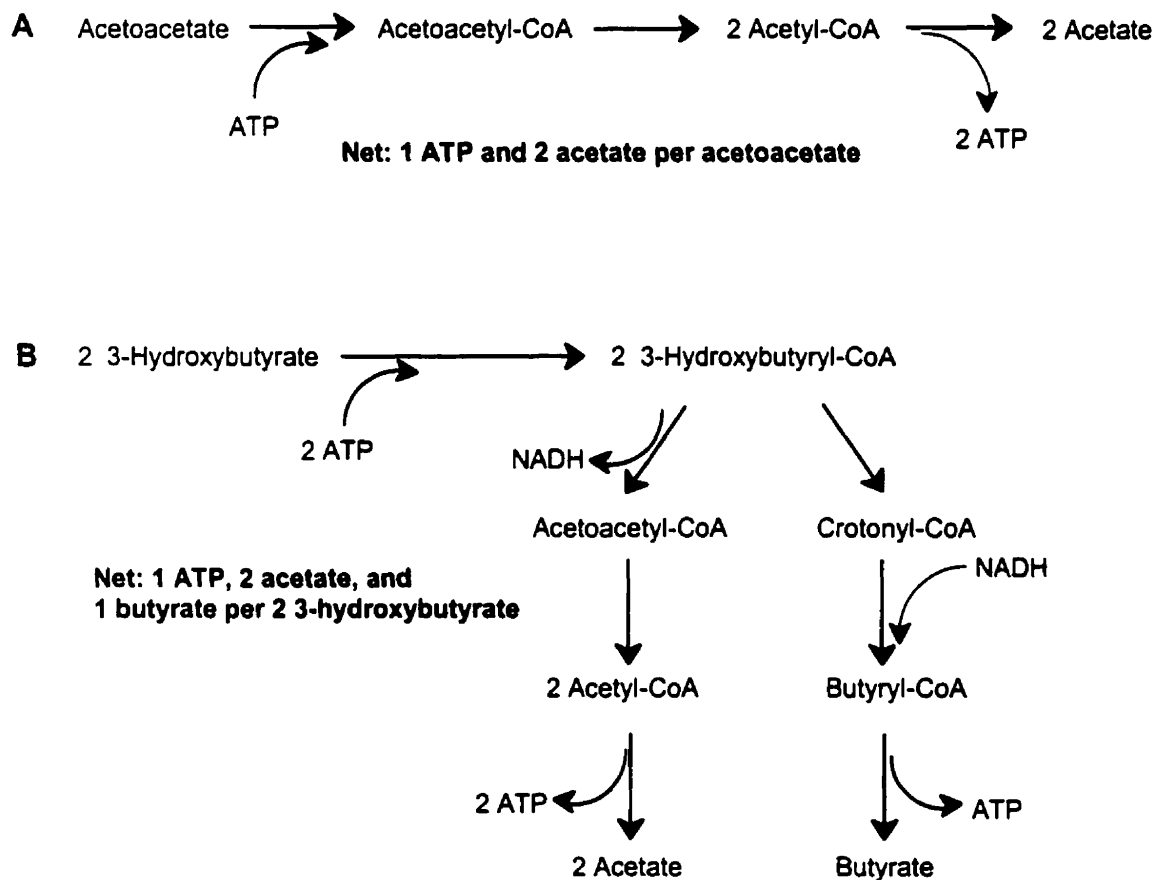
2 Acetate   Butyrate

Figure 2. Energetics and end-product production from the catabolism of the acid forms of the acetate-butyrate pathway intermediates. (A) Acetoacetate and (B) 3-hydroxybutyrate. Crotonate differs from 3-hydroxybutyrate only in the addition of water, so their energy production and end-products should in principal be the same.

1.4   Catabolism of Glutamate

Glutamate degradation by anaerobes produces only one mole of CO_2 per mole of glutamate, whereas aerobic catabolism fully oxidizes glutamate to five moles of CO_2.[28] Sparked by these differences in anaerobic versus aerobic catabolism, various studies on glutamate catabolism using isotopes have been conducted. Two major routes of glutamate degradation have been proposed.

1.4.1   Methylaspartate Pathway of Glutamate Degradation

Initially studied in the anaerobic *Clostridium tetanomorphum*, the methylaspartate pathway (Figure 3) is characterized by the degradation of glutamate into C_2 and C_3 units followed by decarboxylation of the C_3 unit.[28] Feeding experiments with L-[5-^{14}C]glutamate produced $^{14}CO_2$, while the ^{14}C label from L-[1-^{14}C]glutamate and L-[2-^{14}C]glutamate was found in acetate. Atoms C-1 and C-2 of glutamate are converted to acetate, and C-5 is converted to CO_2. Radioactivity was also recovered in butyrate. However, the fermentation of one mole of glutamate produces more than one mole of acetate, suggesting that acetate must also arise from not only atoms C-1 and C-2, but also atoms C-3 and C-4. The formation of butyrate was suggested to proceed via the combination of two acetate units. The ^{14}C label from a L-[4-^{14}C]glutamate experiment was incorporated into the end-products; the recovered butyrate contained twice the specific radioactivity of acetate, and the ^{14}C label in butyrate was symmetrically distributed with equal quantities at C-1 and C-3. In addition, feeding experiments
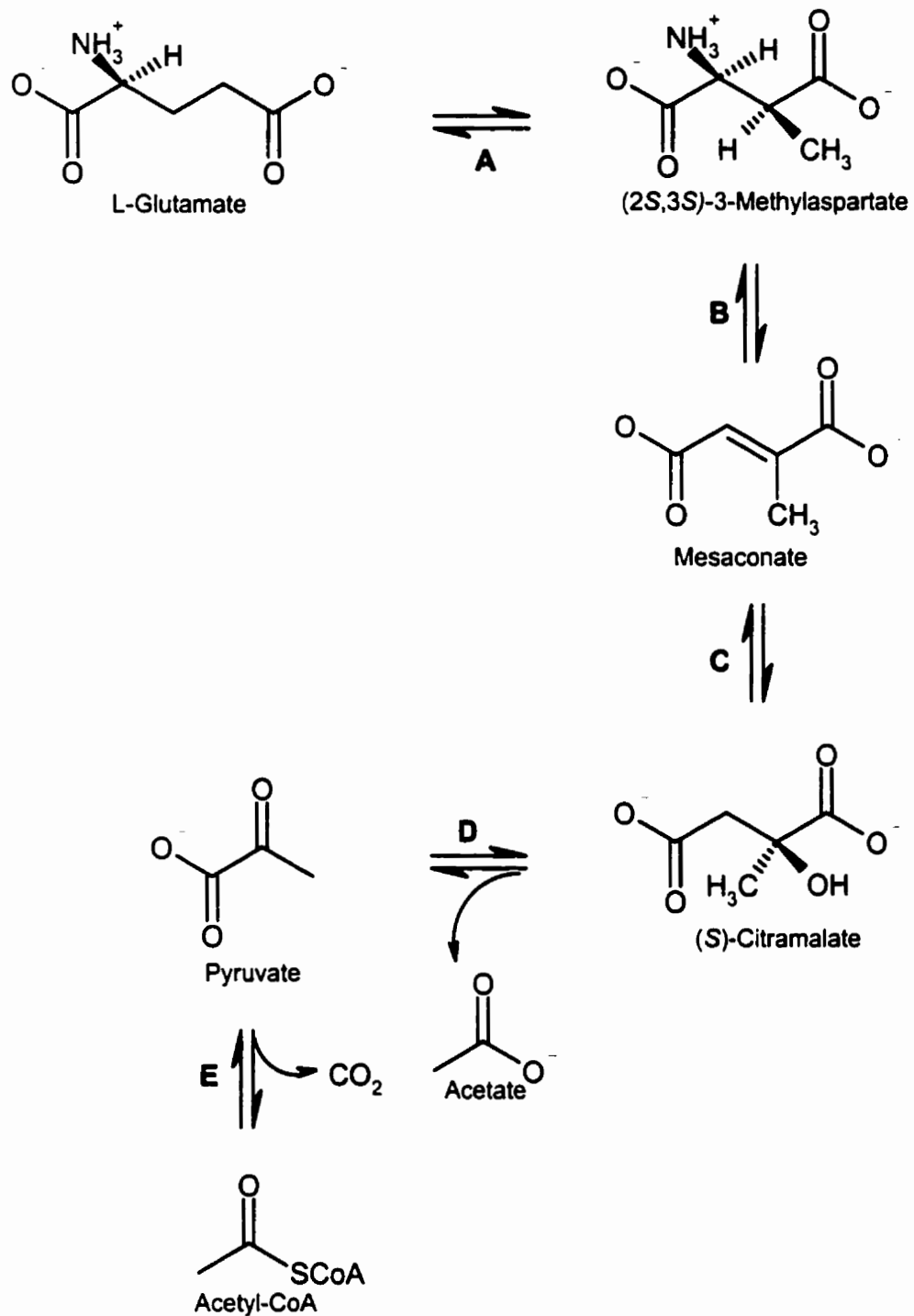
Figure 3. Methylaspartate pathway of glutamate catabolism. (A) Glutamate mutase (EC 5.4.99.1). (B) β-Methylaspartase (EC 4.3.1.2). (C) Mesaconase (EC 4.2.1.34). (D) Citramalate lyase (EC 4.1.3.22). (E) Pyruvate dehydrogenase (EC 1.2.4.1).

with unlabelled glutamate and L-[1-^{14}C]acetate also produced butyrate symmetrically labelled at C-1 and C-3.[29]

The intermediates associated with the methylaspartate pathway were proposed following various studies with cell-free *C. tetanomorphum* extracts. Defining the pathway is the key intermediate (2S,3S)-*threo*-β-methylaspartate,[30] which is formed from L-glutamate by a coenzyme-B$_{12}$-dependent rearrangement catalysed by glutamate mutase (Figure 3, Step A).[31,32] Glutamate mutase has been purified and its gene cloned in *C. tetanomorphum*[33,34,35] and *C. cochlearium*.[36,37] Other enzymes include β-methylaspartase (Figure 3, Step B), which has been mechanistically characterized[38,39,40,41,42] and its gene cloned[43] in *C. tetanomorphum*; citramalate hydrolyase (Figure 3, Step C), dependent on Fe^{2+} and cysteine for the hydration of mesaconate to (S)-citramalate;[28,44,45,46] citramalate lyase (Figure 3, Step D), dependent on divalent cations for the cleavage of (S)-citramalate to pyruvate and acetate;[47,48] and pyruvate dehydrogenase (Figure 3, Step E) for the oxidative decarboxylation of pyruvate to acetyl-CoA.[28] To recycle the NADH formed from oxidative decarboxylation, acetate is converted to butyrate by the acetate-butyrate pathway (Figure 1) using acetate or acetyl-CoA as the entry point.

More recently, the methylaspartate pathway has been identified as the exclusive pathway of glutamate degradation in *F. varium*.[26] In addition to isotopic evidence, glutamate mutase acvitity[26] has been detected and methylaspartase has been purified.[49] A glutamate racemase[26] has also been detected and probably accounts for the ability of *F. varium* to utilize D-glutamate from complex medium without the requirement of a separate pathway for the D-isomer.

The main feature of the methylaspartate pathway is the degradation of glutamate directly to two independent C_2 units, limiting butyrate formation to the combination of C_2 units.

1.4.2 Hydroxyglutarate Pathway of Glutamate Degradation

Unlike the methylaspartate pathway, which degrades glutamate into acetate units, the hydroxyglutarate pathway[50] (Figure 4) degrades glutamate to crotonyl-CoA, an intermediate of the acetate-butyrate conversion pathway (Figure 1). Butyrate can be formed directly from crotonyl-CoA through reduction and CoA transfer reactions. Hence, butyrate would be retained as an intact C_4 unit directly from glutamate. On the other hand, acetate must be formed from the cleavage of crotonyl-CoA.

Enzymes and intermediates in the hydroxyglutarate pathway include NAD+-dependent glutamate dehydrogenase[51,52] (Figure 4, Step A), for the oxidative deamination of L-glutamate to 2-ketoglutarate; (*R*)-2-hydroxyglutarate dehydrogenase[53,54] (Figure 4, Step B), for reduction to (*R*)-2-hydroxyglutarate;[55]

(R)-2-hydroxyglutarate dehydratase[56,57] (Figure 4, Step C), for dehydration to glutaconate; glutaconate:acetyl-CoA CoA-transferase[58] (Figure 4, Step D), for the conversion of glutaconate to its CoA thiol ester; and biotin-dependent glutaconyl-CoA decarboxylase[27,56,59] (Figure 4, Step E), for decarboxylation to crotonyl-CoA.
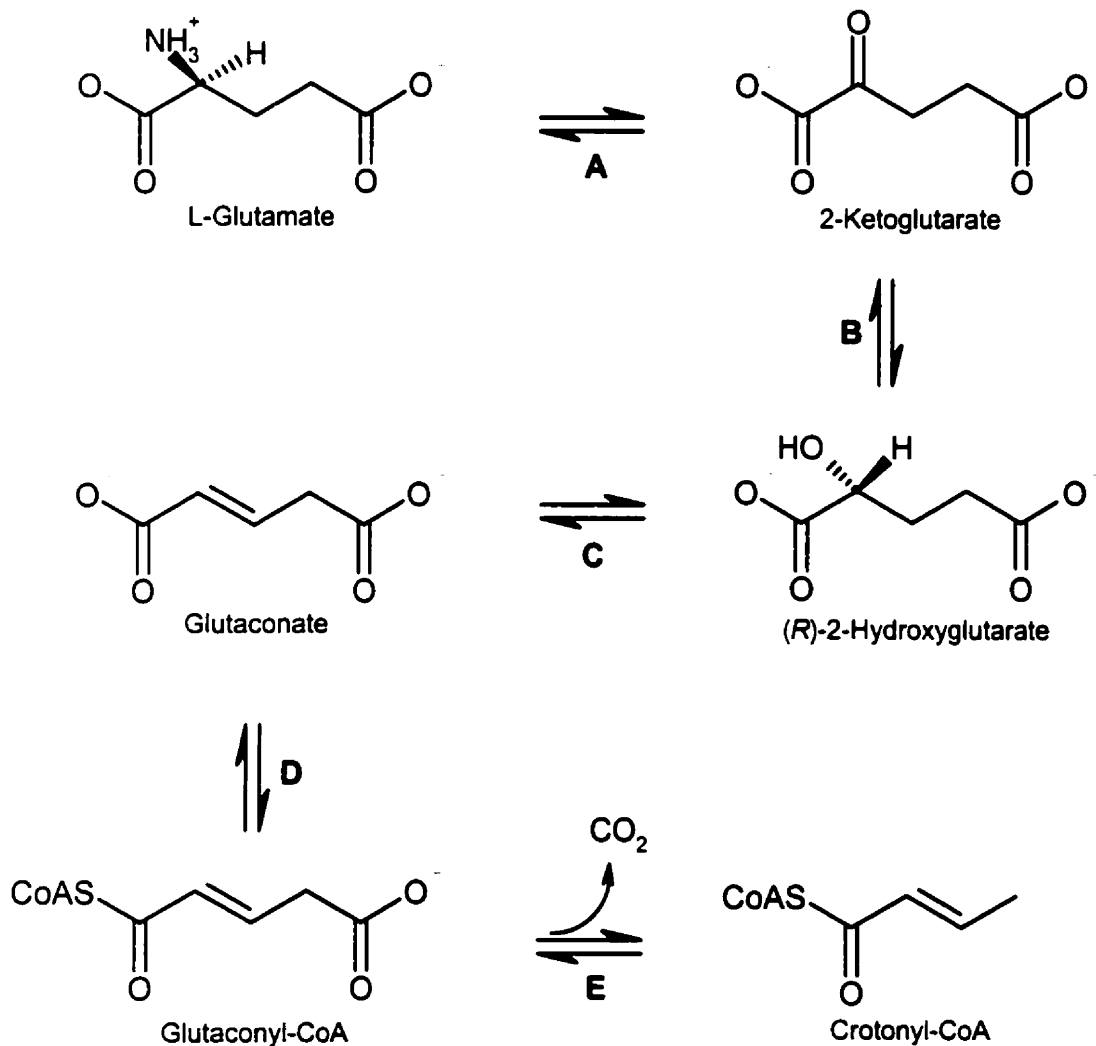
Figure 4. Hydroxyglutarate pathway of glutamate catabolism. (A) Glutamate dehydrogenase (EC 1.4.1.2). (B) 2-Hydroxyglutarate dehydrogenase (EC 1.1.99.1). (C) 2-Hydroxyglutarate dehydratase (EC 4.2.1.-). (D) Glutaconate:acetyl-CoA CoA-transferase (EC 2.8.3.12). (E) Glutaconyl decarboxylase (EC 4.1.1.67).

The hydroxyglutarate pathway was first noticed in *Micrococcus aerogenes*,[60,61] when feeding experiments with L-[1-^{14}C]glutamate demonstrated that the ^{14}C label was found mainly in C-1 of butyrate with a small amount in C-3. Similarly, with L-[2-^{14}C]glutamate, more ^{14}C was found in C-2 than C-4 of butyrate. These labelling asymmetries were inconsistent with the methylaspartate pathway, where a symmetrical distribution of ^{14}C label would have been expected. It was hypothesized that butyrate was formed from glutamate as an intact C$_4$ unit. When DL-[3,4-^{14}C]glutamate was administered, greater quantities of the ^{14}C labels were located at atoms C-3 and C-4 of butyrate than at C-1 and C-2.

Compared to the catabolism of glutamate by *F. varium*, glutamate catabolism in *F. nucleatum* has been studied more extensively. Similar results consistent with the hydroxyglutarate pathway were obtained when the radioactively labelled substrates used in the *M. aerogenes* experiments were administered to *F. nucleatum*,[50] and atom C-5 of glutamate was degraded to CO_2.[62] A confirmatory study using stable ^{13}C isotopes yielded similar results and ruled out the possibility of other pathways.[26,63] Several enzymatic studies have also been performed in *F. nucleatum*.[50,58,62,64,65]

The formation of butyrate as an intact C_4 unit from glutamate is predicted by the hydroxyglutarate pathway, but no isotopic evidence has linked the pathway to the production of an intact C_4 unit. The combination of C_2 units to form butyrate is also a possibility, giving two distinct routes for butyrate formation in *F. nucleatum*.

1.4.3 Catabolism of Histidine via Glutamate as an Intermediate

The degradation of histidine involves a series of several reactions (Figure 5) that convert histidine to glutamate. However, these reactions are not unique to anaerobic bacteria and are also found in aerobic bacteria and mammals.[28]

Since the reactions and enzymes associated with the conversion of histidine to glutamate (Figure 5) are present in advanced organisms such as humans, they have been studied to a greater extent than the enzymes unique to anaerobes.

The first reaction in the degradation of histidine involves the conversion of L-histidine to trans-urocanate, catalyzed by histidine ammonia-lyase (HAL; Figure 5, Step A). In humans, HAL deficiencies have been associated with histidinemia, a genetic disease found in French Canadians in a localized region of Quebec at a rate of 1/4000 births.[66] HAL is functionally and structurally related to phenylalanine ammonia-lyase (PAL),[67] and its crystal structure has been determined.[68]
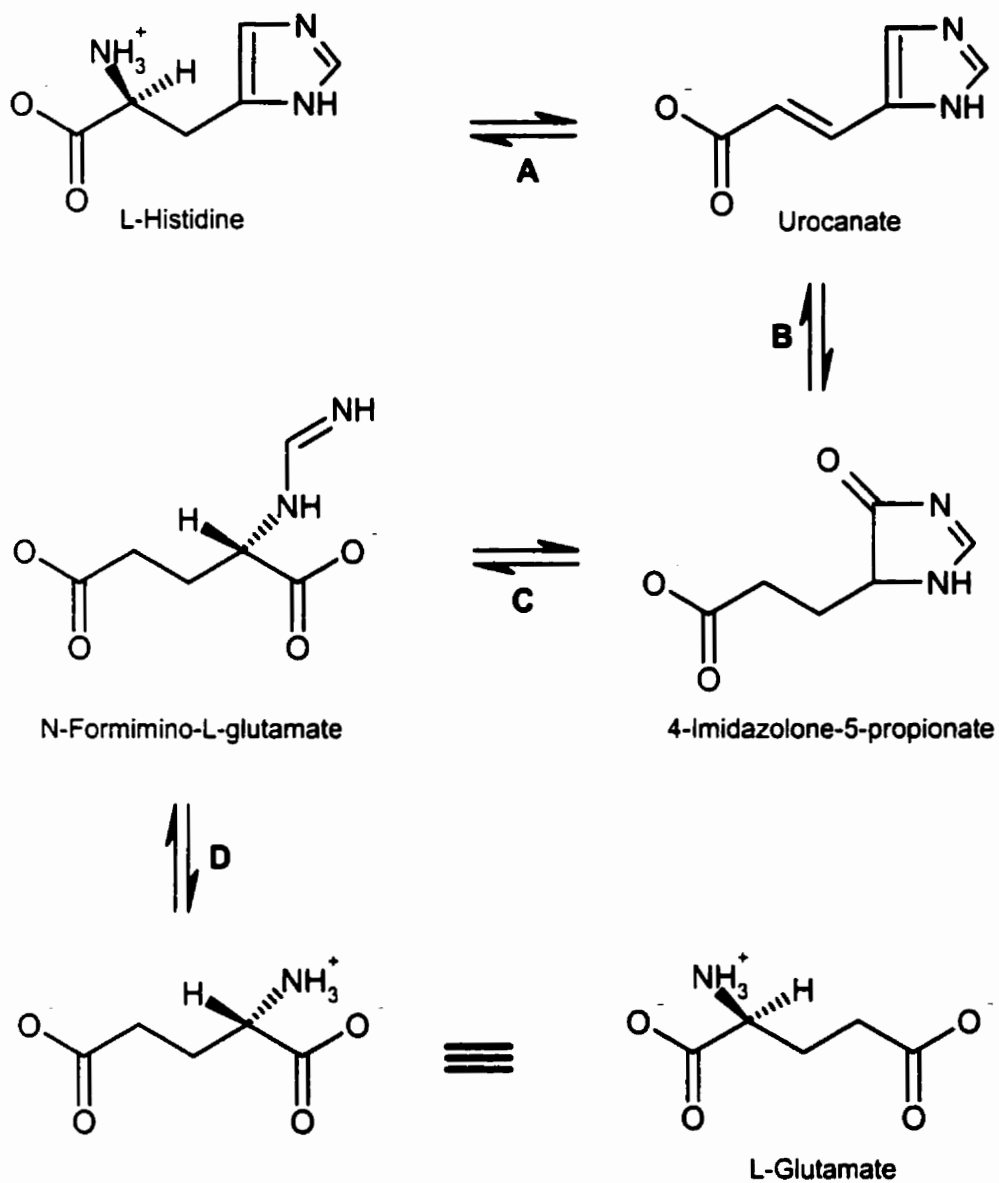
Figure 5. Conversion of histidine to glutamate by anaerobic and aerobic organisms. (A) Histidine ammonia-lyase (EC 4.3.1.3). (B) Urocanate hydratase (EC 4.2.1.49). (C) Imidazolone-propionase (EC 3.5.2.7). (D) Glutamate formiminotransferase (EC 2.1.2.5). Note that the α-carbon of glutamate is derived from the γ-carbon of histidine.

Urocanate undergoes water addition in the second step of the reaction to form 4-imidazolone-5-propionate, catalyzed by urocanate hydratase (Figure 5, Step B). This is the first enzyme known to use NAD^+ as an electrophile rather than an oxidizing agent.[69]

Imidazolonepropionase (Figure 5, Step C) then hydrolyzes a C-N bond in 4-imidazolone-5-propionate, breaking the cyclic imidazole ring to form N-formimino-L-glutamate.[70] A final reaction converts N-formimino-L-glutamate to L-glutamate via glutamate formiminotransferase (Figure 5, Step D). Transfer of the formimino group to the required cofactor tetrahydrofolate produces 5-formiminotetrahydrofolate.[71] The formimino group is released as formamide and hydrolysed to formate.

In anaerobic bacteria, the glutamate produced from histidine would be catabolized via the methylaspartate or the hydroxyglutarate pathway. However, histidine metabolism in *Fusobacterium* species has not been investigated, so its degradation to glutamate cannot be assumed.

1.5 Catabolism of Lysine

While several studies on glutamate catabolism have been carried out in *F. nucleatum* and *F. varium*, relatively little information pertaining to lysine catabolism is available. In fact, there is no literature information on lysine catabolism by *F. varium*, and the information presented for *F. nucleatum* is inconclusive.[23]

However, lysine catabolism in the anaerobic *Clostridium* species has been investigated[72] more thoroughly, and the information available may also be applicable to *Fusobacterium*. Isotopic and enzymatic studies have suggested that the D- and L-isomers of lysine are degraded via separate pathways, even though a lysine racemase may be present for the interconversion of the two isomers. The possibility of the two distinct pathways has been extended to *F. nucleatum*,[23] despite the lack of concrete evidence.

1.5.1 Catabolism of L-Lysine via the 3,5-Diaminohexanote Pathway

Catabolism of D- and L-lysine by clostridia results in the formation of butyrate, acetate, and ammonia,[73,74] although the two isomers are degraded via different pathways. A complete pathway for L-lysine[72,75] (Figure 6) has been proposed.

Degradation of L-lysine requires six enzymatic reactions to produce two intermediates of the central acetate-butyrate pathway (Figure 1), acetoacetyl-CoA and crotonyl-CoA. The first enzymatic reaction by L-lysine-2,3-aminomutase (Figure 6, Step A) rearranges the α-amino group in L-lysine to produce (S)-β-lysine. The *Clostridium* enzyme has been characterized[76,77] and the gene cloned,[78] and is dependent on the cofactors pyridoxal phosphate, Fe^{2+}, (S)-adenosylmethionine for the radical-based rearrangement.
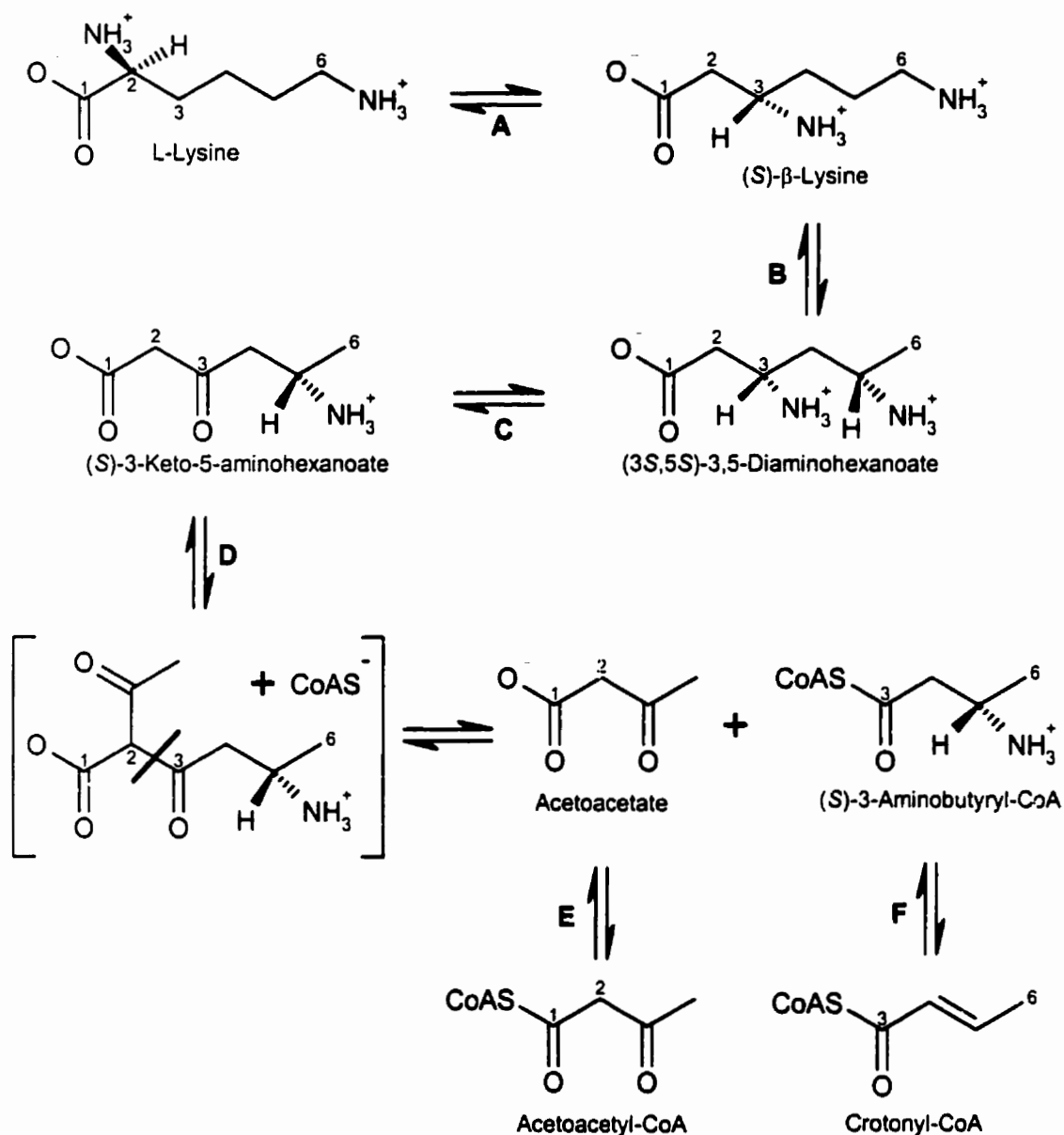
Figure 6. Catabolism of L-lysine by *Clostridium* species via the 3,5-diaminohexanoate pathway. Numbers represent the carbon atoms in lysine. (A) Lysine-2,3-aminomutase (EC 5.4.3.2). (B) β-Lysine mutase (EC 5.4.3.3). (C) 3,5-Diaminohexanoate dehydrogenase (EC 1.4.1.11). (D) 3-Keto-5-aminohexanoate cleavage enzyme. (E) Butyryl-CoA:acetoacetate CoA-transferase (EC 2.8.3.9). (F) (*S*)-3-Aminobutyryl-CoA deaminase (EC 4.3.1.14)

(S)-β-Lysine is subsequently converted to (3S,5S)-3,5-diaminohexanoic acid via the rearrangement of the ε-amino group (Figure 6, Step B) by β-lysine mutase.[79,80] A variety of cofactors[81,82] are required for the rearrangement, including pyridoxal phosphate, coenzyme B_{12}, ATP, a thiol, pyruvate, and monovalent and divalent cations.

Oxidative deamination of (3S,5S)-3,5-diaminohexanoic acid to (S)-3-keto-5-aminohexanoic acid (Figure 6, Step C) is catalyzed by NAD^+-dependent 3,5-diaminohexanoate dehydrogenase.[83,84] Ammonia and NADH are also products of the reaction; NADH is later recycled to NAD^+ in the reduction of crotonyl-CoA to butyryl-CoA.

Cleavage of the C_6 (S)-3-keto-5-aminohexanoic acid into acetoacetate and (S)-3-aminobutyryl-CoA (Figure 6, Step D) is catalyzed by the 3-keto-5-aminohexanoic acid cleavage enzyme.[85] A unique feature is a C_8 intermediate that is postulated to be formed via a Claisen condensation with acetyl-CoA; subsequent retro-Claisen cleavage forms two C_4 units. The lysine backbone within the C_8 intermediate is cleaved between C-2 and C-3 of lysine.

The two C_4 units are then converted to intermediates in the central acetate-butyrate pathway. Acetoacetate is converted to acetoacetyl-CoA via butyryl-CoA:acetoacetate CoA-transferase[86] (Figure 6, Step E) before cleavage and then via thiolase (Figure 1) to acetyl-CoA. Deamination of (S)-3-aminobutyryl-CoA to crotonyl-CoA proceeds via (S)-3-aminobutyryl-CoA deaminase[87] (Figure 6, Step F).

1.5.2   Catabolism of D-Lysine via the 2,5-Diaminohexanoate Pathway

The degradation of D-lysine is proposed to proceed via a pathway (Figure 7) separate from that of L-lysine. However, only two steps have been proposed based on detected enzyme activities.[72]

The first enzymatic reaction involves the rearrangement of the ε-amino group in D-lysine to (2R,5?)-2,5-diaminohexanoic acid by D-α-lysine mutase (Figure 7, Step A); rearrangement of the α-amino group does not occur, and the stereochemistry at C-5 has not been established. The similarities between D-α-lysine mutase in the D-pathway and β-lysine mutase in the L-lysine pathway (Figure 6, Step B) have suggested that the two enzymes are actually two interconvertible forms of one enzyme.[72] Cofactors required for D-α-lysine mutase activity include pyridoxal phosphate, coenzyme B_{12}, and ATP.[88,89]

Subsequent oxidative deamination of the diaminohexanoic acid to (R)-2-amino-5-ketohexanoic acid occurs via 2,5-diaminohexanoate dehydrogenase (Figure 7, Step B). It is interesting to note that this enzyme has a greater activity towards 2,4-aminopentanoic acid, an intermediate formed in the catabolism of the amino acid ornithine; 2,5-diaminohexanoate dehydrogenase is perhaps the same enzyme found in the ornithine pathway, 2,4-diaminopentanoate dehydrogenase.[72] The product, 2-amino-5-ketohexanoic acid, undergoes spontaneous reversible cyclization (Figure 7, Step C) and can be isolated as Δ^1-pyrroline-2-methyl-5-carboxylic acid.
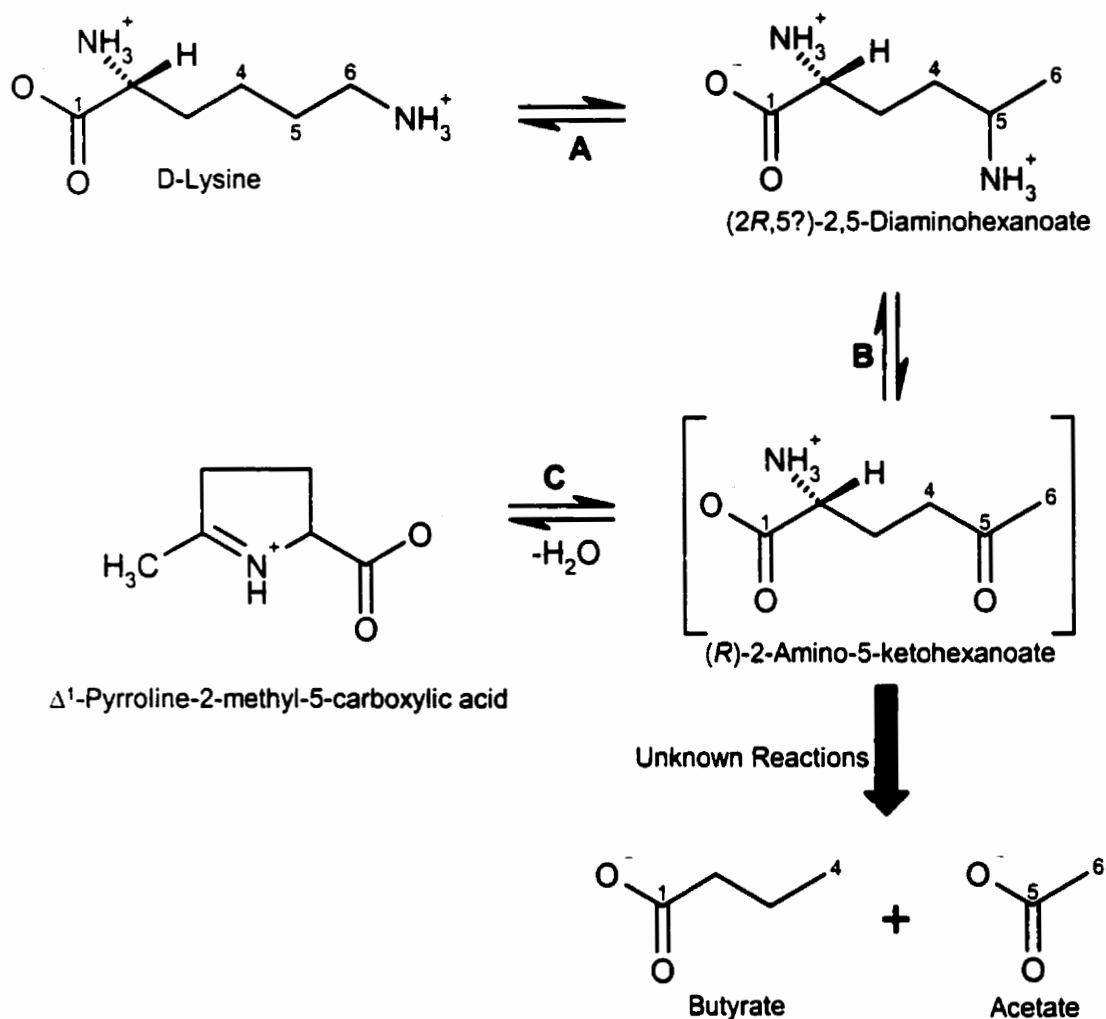
Figure 7. Catabolism of D-lysine by *Clostridium* species via the 2,5-diaminohexanoate pathway. Numbers refer to the carbon atoms of lysine. (A) D-α-Lysine mutase (EC 5.4.3.4). (B) 2,5-Diaminohexanoate dehydrogenase, possibly identical to 2,4-diaminopentanoate dehydrogenase (EC 1.4.1.12). (C) Spontaneous.

Further steps in the pathway have not been elucidated. The stages in the conversion of 2-amino-5-ketohexanoic acid to the end-products are unknown, but thiolytic cleavage between atoms C-4 and C-5 has been suggested.[72]

The most significant differences between the D- and L-lysine pathways lie in the bond at which the lysine backbone is cleaved. Cleavage of L-lysine occurs between atoms C-2 and C-3, producing butyrate derived from lysine atoms C-3 to C-6. On the other hand, cleavage of D-lysine between atoms C-4 and C-5 generates butyrate derived from atoms C-1 to C-4. Nonetheless, in both pathways, butyrate is theoretically derived from an intact C_4 unit originating from lysine.

1.5.3   Lysine Racemase

The occurrence of a lysine racemase for the interconversion of D- and L-lysine has not been established in *Fusobacterium* species. Generally speaking, little information regarding lysine racemases exist in the literature. For instance, in anaerobic bacteria, lysine racemase activity has been detected using linked assays in the cell-free extracts of *Clostridium*,[76] but the enzyme has not been purified and characterized. In aerobes, a plasmid carrying the lysine racemase gene has been found in *Pseudomonas putida*,[90] while lysine racemase has been implicated in *Streptomyces clavuligerus* based on the ability of D-lysine to stimulate β-lactam antibiotic production.[91]

1.5.4   Catabolism of D- and L-Lysine in *F. nucleatum*

Of all the *Fusobacterium* species, lysine catabolism has only been studied in *F. nucleatum*.[23] Using isotopically labelled substrates and through the assay of the enzymes associated with the L-lysine catabolism, it was concluded that the pathway of L-lysine degradation in *F. nucleatum* is similar to the pathway found in *Clostridium*. Yet, the evidence for the degradation of D-lysine via the same D-pathway present in *Clostridium* is inconclusive: no enzymatic activities related to the D-lysine pathway were detected, and the conclusion that a separate D-pathway is present was based on the results of isotopic feeding experiments using a racemic mixture. A brief summary of the three experiments is outlined.

An initial feeding experiment was carried out by incubating *F. nucleatum* with [1-^{14}C]acetate in the presence of unlabelled L-lysine. The acetate and butyrate end-products were isolated and their specific radioactivities determined. Butyrate contained approximately twice the specific radioactivity of acetate, confirming the presence of the acetate-butyrate pathway that converts two acetate units into a single butyrate (Figure 1). More importantly, an asymmetric distribution of ^{14}C was observed in butyrate; C-3 was enriched to a greater extent than C-1 (42% and 55% distribution, respectively). The asymmetric distribution supports the unique C_8 intermediate in the pathway of L-lysine catabolism, indicating similarities with the *Clostridium* species. However, it must be considered that the differences in the distribution are not very large (42% versus 55%).

A second experiment was performed by incubating *F. nucleatum* with DL-[1-^{14}C]lysine and unlabelled L-lysine. The recovered butyrate contained a C-1:C-3 ^{14}C distribution of 62:38, indicating that C-1 of butyrate is derived from C-1 of lysine. However, this experiment used a racemic mixture of [1-^{14}C]lysine. Atom C-1 of butyrate can be derived directly from the D-lysine pathway (Figure 7) if the labelled lysine is cleaved between atoms C-4 and C-5. Similarly, if cleavage between C-2 and C-3 occurred as in the L-lysine pathway (Figure 6) and the acetoacetate formed proceeded to butyrate, the label would still be located at atom C-1 of butyrate. That is, with the use of a racemic labelled mixture, the concurrent operation of both pathways or either pathway on its own can produce butyrate with a higher enrichment at C-1. The smaller amount of label located at C-3 of butyrate is caused by the constant interconversion of acetoacetate and acetate.

In a third experiment, *F. nucleatum* was incubated with DL-[6-^{14}C]lysine in the presence of unlabelled L-lysine. Results are complementary to those obtained in the second experiment; the label was mainly at C-4 of butyrate (81%) in addition to C-2 (18%). Cleavage of the L-isomer of DL-[6-^{14}C]lysine between C-2 and C-3 forms butyrate labelled at C-4. However, the coupling of two labelled acetates formed from the D-pathway or from a C$_4$ intermediate of the L-pathway would provide labelling at both C-2 and C-4 of butyrate. Once again, the results are inconclusive.

Based on these inconclusive studies, it was still suggested that the pathways of D- and L-lysine catabolism in *F. nucleatum* are similar to those of the *Clostridium* species.[23] Further studies with stereochemically pure labelled lysine samples should provide more convincing results.

1.6   Outline and Proposal of Research Objectives

Ideally, amino acid catabolism should be studied in the absence of other substrates and potential interferences. Since complex medium is of undefined composition, it would be preferential to study amino acid catabolism by resuspending the bacterial cells in a buffer solution, free of other carbon sources. Not only would the interferences be eliminated, but the identification and isolation of end-products would be also simplified. Whether amino acids are efficiently catabolized by cell resuspensions, however, needs to be determined.

The acetate-butyrate pathway (Figure 1) will also be studied in greater detail to determine whether the acid forms of the intermediates can be taken up by the bacterial cells and catabolized to end-products. If consumption of the substrates occurs, their relative rates and product ratios can be compared to their theoretical values.

The remainder of the thesis focuses on the catabolism of the amino acids glutamate, histidine, and lysine. Initial studies will determine whether butyrate is formed directly from the amino acids as an intact C_4 unit (Figures 4, 6, and 7) or is derived from the combination of two acetate-derived C_2 units (Figures 1 and 3).

That is, whether the entry points into the acetate-butyrate pathway are C_2 or C_4 intermediates can be determined. These two modes of butyrate formation can be distinguished using universally ^{13}C-labelled amino acids (Figure 8), and analysis of the labelled butyrate can be determined by ^{13}C-NMR spectroscopy.

However, it must first be demonstrated that any $[^{13}C_4]$butyrate formed directly from a $[U^{-13}C]$amino acid (Figure 8, Route A) will remain at detectable levels and not undergo cleavage to acetate units to an appreciable extent (Figure 8, Route C). Secondly, the extent of $[^{13}C_4]$butyrate formation by the combination of $[^{13}C_2]$acetate units (Figure 8, Route C) must be established. Clearly, the combination of the latter must be small relative to the former, if the detection of $[^{13}C_4]$butyrate is to demonstrate the transfer of four contiguous carbon atoms from the amino acid to butyrate.

As shown in Figure 9, $[^{13}C_4]$-, $[1,2^{-13}C_4]$-, $[3,4^{-13}C_4]$-, and unlabelled butyrate are the possible products when two acetate units in a mixture of $[^{13}C_2]$- and unlabelled acetate are combined. The amount of $[^{13}C_4]$butyrate formed in this process is a statistical reflection of the relative amounts of $[^{13}C_2]$- and unlabelled acetates in the metabolic pool. It is anticipated that the co-administration of unlabelled acetate with the $[U^{-13}C]$amino acid will significantly reduce the synthesis of $[^{13}C_4]$butyrate from $[^{13}C_2]$acetate. Statistically, a two-fold increase in the intracellular concentration of unlabelled acetate would reduce the odds of $[^{13}C_4]$butyrate by four-fold.
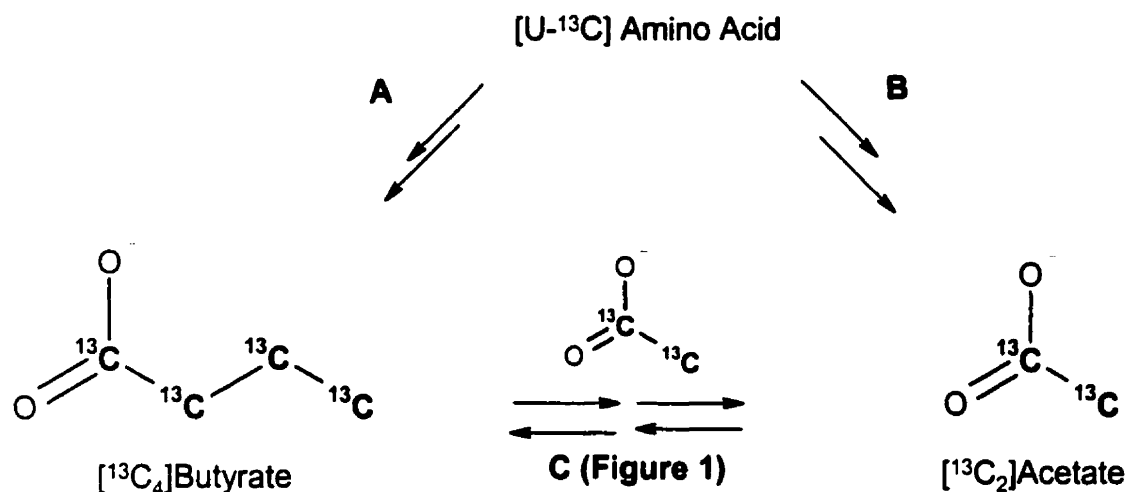
Figure 8. Possible routes of [$^{13}C_4$]butyrate formation from amino acids. (A) Direct formation from the universally ^{13}C-labelled amino acid as an intact four-carbon unit. (B) Degradation of the amino acid into [$^{13}C_2$]acetate. (C) The combination and interconversion of two [$^{13}C_2$]acetate units.

Glutamate catabolism by the hydroxyglutarate pathway in *F. nucleatum* (Figure 4) and by the methylasparate pathway in *F. varium* (Figure 3) correspond to Routes A and B, respectively, in Figure 8. Based on these differences, the validity of this approach can be established in glutamate experiments and then used to determine the mode of butyrate formation from histidine and lysine in the two *Fusobacterium* species.
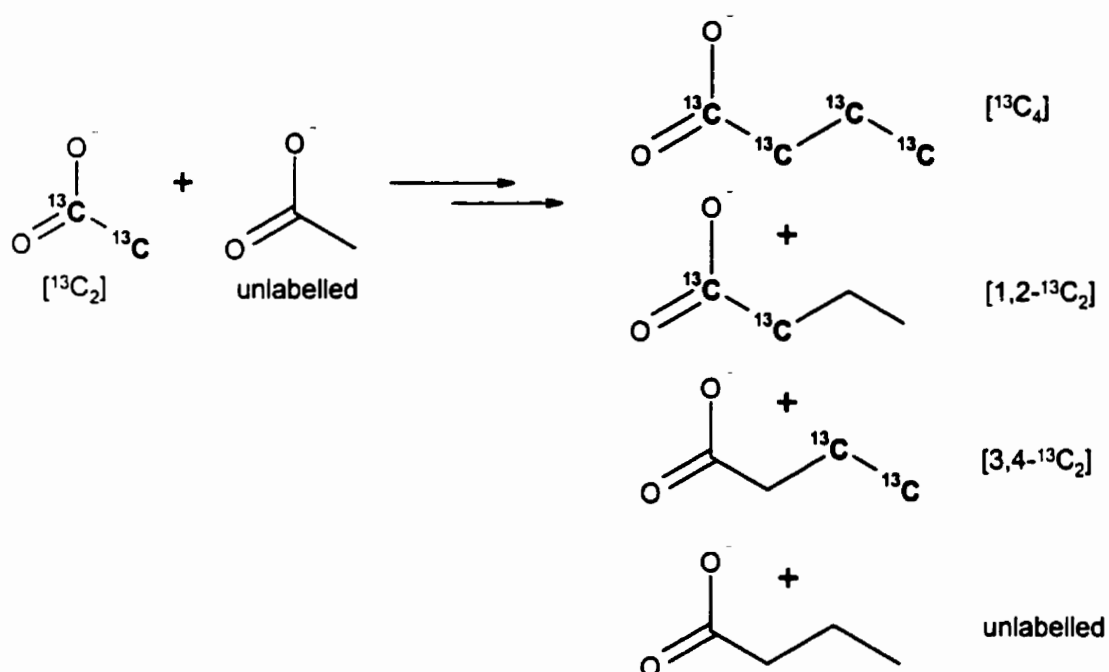
Figure 9. Possible combinations of [$^{13}C_2$]- and unlabelled acetates to form [$^{13}C_4$]-, [1,2-$^{13}C_4$]-, [3,4-$^{13}C_4$]-, and unlabelled butyrates.

Once the route of butyrate formation has been established, the possibility of dual pathways in the catabolism of lysine can be investigated in the two *Fusobacterium* species. The use of $^{13}C_2$-labelled stereochemically pure lysine will provide unambiguous evidence for the presence of two pathways, one for each stereoisomer, or for one pathway and a lysine racemase.

Chapter 2: Substrate Metabolism by Cell Resuspensions

2.1   Amino Acid Catabolism by *Fusobacterium* Resuspensions

Prior to the investigation of the metabolic pathways using isotopically labelled substrates, the utilization of the amino acids glutamate, histidine, and lysine by PBS resuspensions of *F. nucleatum* and *F. varium* was examined. By using buffered resuspensions as opposed to complex medium, the catabolism of the amino acids into end-products could be studied without interferences from any other carbon sources present in the initial complex medium. Competition effects from other substrates in the medium are also eliminated. In separate experiments, decreases in glutamate, histidine and lysine concentrations were monitored by HPLC over time, and at the end of the incubation period, the acidic end-products were isolated as sodium salts and identified by ^{1}H-NMR spectroscopy (Table 1).

Utilization of glutamate, histidine, and lysine by both organisms was observed within 2-24 h of incubation (Table 1). L-Glutamate was utilized rapidly by both organisms, but the relative rates of histidine and lysine assimilation differed in *F. nucleatum* and *F. varium*. In *F. nucleatum*, the rate of histidine catabolism was slower than that of glutamate but faster than that of lysine. In *F. varium*, on the other hand, the rate of lysine utilization was comparable to that of glutamate, whereas histidine catabolism was noticeably slower.

29

Table 1. Utilization of amino acids by F. nucleatum and F. varium.

Amino Acid (10 mM)	Organism	Time (h)	Residual Amino Acid (%) [a]	Relative amounts [b] amino acid : acetate : butyrate : formate
None	F. nucleatum	10	--	Trace amount of acetate
None	F. varium	24	--	Trace amount of acetate
D-Glutamate	F. nucleatum	24	79	3.4 : 2.3 : 1.0 : nd
L-Glutamate	F. nucleatum	2.5	0	nd : 2.1 : 1.0 : nd
D-Glutamate	F. varium	2.5	4	nd : 2.1 : 1.0 : nd
L-Glutamate	F. varium	2.5	0	nd : 2.0 : 1.0 : nd
D-Histidine	F. nucleatum	10	2	nd : 2.1 : 1.0 : 0.7
L-Histidine	F. nucleatum	10	0	nd : 1.9 : 1.0 : 1.0
D-Histidine	F. varium	24	43	2.3 : 2.0 : 1.0 : 0.7
L-Histidine	F. varium	24	9	0.2 : 1.9 : 1.0 : 0.7
D-Lysine	F. nucleatum	10	24	0.4 : 1.2 : 1.0 : nd
L-Lysine	F. nucleatum	10	13	0.2 : 1.0 : 1.0 : nd
D-Lysine	F. varium	2.5	10	0.1 : 1.2 : 1.0 : nd
L-Lysine	F. varium	2.5	0	nd : 1.1 : 1.0 : nd

[a] Determined by HPLC and expressed as a percentage of the original concentration
[b] Determined by ^{1}H-NMR spectroscopy; nd = not detected

In all cases, the L-amino acids were utilized more rapidly than the corresponding D-isomers, which may indicate the presence of amino acid racemases. While this utilization pattern is similar to that shown by cells growing on peptone medium,[19] the slow utilization of D-glutamate and D-histidine by F. nucleatum and F. varium resuspensions, respectively, was not evident in the previous studies of amino acid uptake from complex medium. The complex medium may have contained other undefined components that were

preferentially catabolized over D-glutamate and D-histidine. These results illustrate the importance of using interference-free PBS resuspensions to assess amino acid catabolism.

In each experiment, acetate and butyrate were identified as end-products by ^{1}H-NMR spectroscopy, and formate was also detected as an end-product of histidine catabolism (Table 1). No other unidentified signals were in observed in the ^{1}H-NMR spectra of lyophilised culture supernatants collected in the glutamate, histidine, and lysine feeding experiments; a sample spectrum is shown in Figure 10. Control experiments indicated that *F. nucleatum* and *F. varium* released only trace amounts of acetate into the resuspension buffer in the absence of any added substrates.

The ratio of the ^{1}H-NMR signals indicated that glutamate and histidine catabolism produced acetate and butyrate in a 2:1 ratio and that equal amounts of these end-products were formed from lysine. Comparable amounts of formate and butyrate accumulated from histidine catabolism. For the experiments in which residual amino acid was detected, the amino acid to butyrate ratio reflects the extent of amino acid utilization determined by HPLC.

These results prompted further studies into the formation of butyrate from the three amino acids by *F. nucleatum* and *F. varium*. Universally labelled ^{13}C amino acids and ^{13}C-NMR spectroscopy were later employed to determine whether butyrate was formed as a intact C_4 unit directly from the amino acids (Chapter 3).
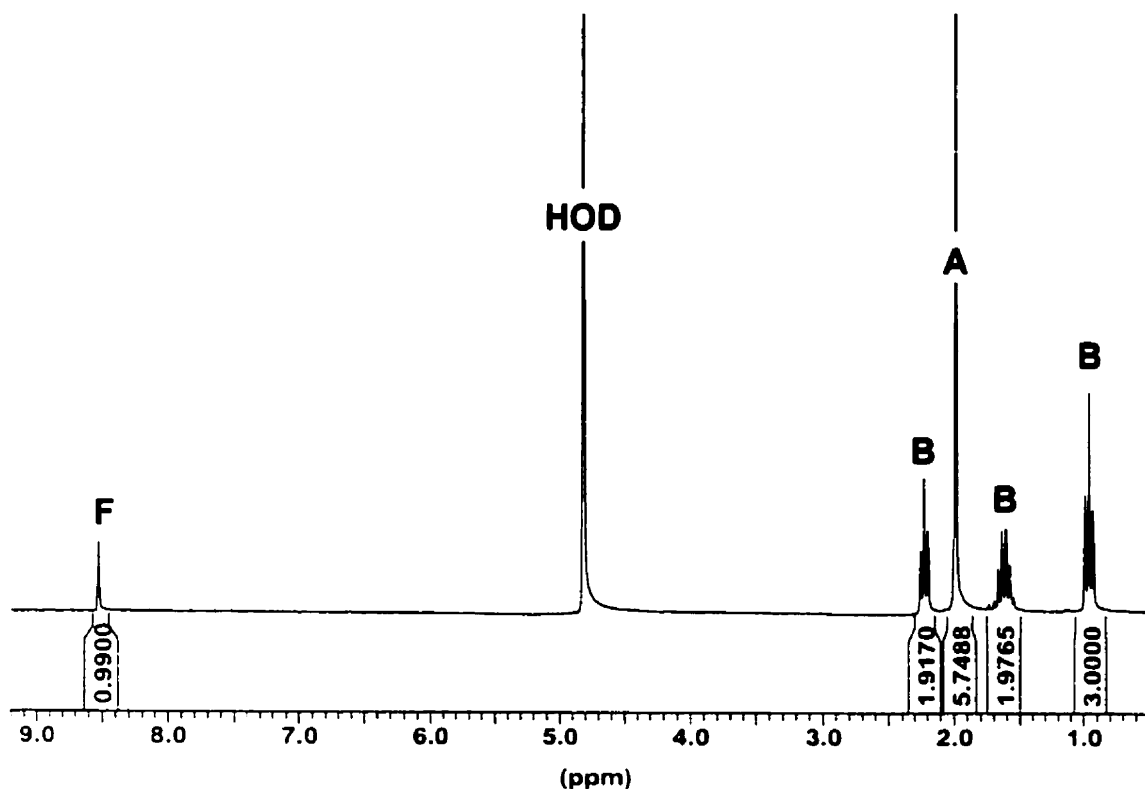
Figure 10. ^{1}H-NMR spectrum (250 MHz) of the end-products of L-histidine catabolism by *F. nucleatum*. Signals are indicated as follows: A, acetate; B, butyrate, F, formate.

2.2 Metabolism of the Unesterfied Forms of the Acetate-Butyrate Pathway Intermediates

The ability of *F. nucleatum* and *F. varium* resuspensions to assimilate the acid forms of the intermediates in the acetate-butyrate pathway (Figure 1) was determined. Similar to the amino acid usage experiments, the end-products were isolated as sodium salts and analyzed by ^{1}H-NMR spectroscopy (Table 2). In

instances where the substrates were consumed, the end-product ratios are comparable to those predicted by the acetate-butyrate pathway (Figure 2). Only acetate and butyrate were detected as end-products, and similar results were observed in both organisms for the four substrates studied (Table 2).

Table 2. Catabolism of the acid forms of the acetate-butyrate pathway intermediates.

Substrate (10 mM)	Organism	Relative amounts [a] substrate : acetate : butyrate
Acetoacetic acid	*F. nucleatum*	0.2 : 1.0 : nd
Acetoacetic acid	*F. varium*	nd : 16.0 : 1.0
Crotonic acid	*F. nucleatum*	1.4 : 1.6 : 1.0
Crotonic acid	*F. varium*	0.3 : 1.5 :1.0
(*R*)-3-Hydroxybutyric acid	*F. nucleatum*	Not catabolized
(*R*)-3-Hydroxybutyric acid	*F. varium*	2.0 : 1.7 : 1.0
(*S*)-3-Hydroxybutyric acid	*F. nucleatum*	nd : 1.8 : 1.0
(*S*)-3-Hydroxybutyric acid	F. varium	0.5 : 1.6 : 1.0

[a] Determined by ^{1}H-NMR spectroscopy; nd = not detected

Acetoacetate was rapidly catabolized by both organisms, producing acetate as the main end-product. The quick catabolism of acetoacetate most likely reflects its close proximity to acetyl-CoA, requiring only one additional enzymatic reaction (Figure 1, Step B) after its converstion to the CoA ester. Since no NADH is formed from this reaction, no recycling to NAD$^+$ by butyrate formation is required. In other words, the conversion of acetate to butyrate is not necessary. Several enzymatic reactions, which may be the slow steps of the conversion sequence, are not required (Figure 1, Steps C-E).

On the contrary, the catabolism of crotonic acid and 3-hydroxybutyrate requires the operation of all reactions in the acetate-butyrate pathway (Figure 1), potentially slowing their catabolism. The production of acetyl-CoA from crotonyl-CoA and 3-hydroxybutyryl-CoA requires NAD^+, and the NADH formed must be recycled by butyrate formation. Small amounts of crotonic acid were detected at the end of the incubation period for both *F. nucleatum* and *F. varium*. However, difficulties in the transportation of crotonic acid into the cell or in the conversion to is CoA ester may also account for its slower usage.

(*R*)-3-Hydroxybutyrate was either not catabolized at all or catabolized slower than its enantiomer, (*S*)-3-hydroxybutyrate. The preferential catabolism of one isomer may suggest that the 3-hydroxybutyryl-CoA intermediate of the acetate-butyrate pathway is of the *S*-isomer. However, a definite conclusion cannot be made, as the feeding experiments were performed using the acid forms of the intermediates instead of the CoA esters. An unidentified enzyme responsible for converting the two enantiomeric acids to their corresponding CoA esters may exhibit greater activity towards the *S*-isomer. Furthermore, enantiomeric specificity may also lie in two other enzymes, hydroxybutyryl-CoA dehydrogenase (Figure 1, Step C) and crotonase (Figure 1, Step D). If these enzymes are stereospecific for the *S*-isomer and exhibit high selectivity, the slow catabolism of the *R*-isomer may be due to a different set of enzymes that act on the *R*-isomer, but at a reduced rate.

In general, the formation of CoA esters from carboxylic acids are usually

catalyzed by transferase enzymes such as butyryl-CoA:acetate CoA-transferase

(Figure 1, Step A) and butyryl-CoA:acetoacetate CoA-transferase (Figure 6, Step

E). These enzymes probably have a broad substrate specificity and may account

for the ability to catabolize the four-carbon acids investigated.

2.3   Catabolism of Acetate Derivatives

The ability of F. nucleatum and F. varium to assimilate two acetate

derivatives, fluoroacetate and acetylNAC, was also investigated (Table 3).

Table 3. Catabolism of acetate derivatives.

Substrate (10 mM)	Organism	Relative amounts [b]
Fluoroacetic acid [a]	F. nucleatum	2.4 : 2.2 : 1.0 fluoroacetate : acetate : butyrate
Fluoroacetic acid [a]	F. varium	2.3 : 2.5 :1.0 fluoroacetate : acetate : butyrate
AcetylNAC	F. nucleatum	Not catabolized
AcetylNAC	F. varium	1.6 : 1.0 : 1.1 AcetylNAC : acetate : NAC

[a]   Incubated with a co-substrate of L-glutamate (10 mM)
[b]   Determined by ^{1}H-NMR spectroscopy; nd = not detected

Fluoroacetate was incubated along with L-glutamate, and if fluoroacetate

were assimilated, the incorporation of fluorine into butyrate should be observed.

The L-glutamate only serves to provide an energy source for the bacterial cells,

so that butyrate can be formed. The presence of fluorine is easily detected by the observation of ^{1}H-^{19}F coupling in the ^{1}H-NMR spectra of the end-products. With both *F. nucleatum* and *F. varium*, no fluorobutyrate was observed. All of the glutamate was metabolized into the end-products acetate and butyrate, with the same ratios as those observed in the absence of fluoroacetate (Table 1). The inability to incorporate fluoroacetate may be attributed to transportation difficulties or to the inability of any one or more of the enzymes in the acetate-butyrate pathway (Figure 1) to function with fluorinated derivatives.

On the other hand, acetylNAC was assimilated, but only by *F. varium*. AcetylNAC metabolism is characterized by the two end-products acetate and NAC (Figure 11). Two routes of acetylNAC metabolism are possible, and are differentiated by acetyl-CoA as an intermediate. In the first route (Figure 11, Route A), acetylNAC is a direct substrate for ATP production, where the NAC ester functions equivalently as though a CoA ester. Whereas, in the second route (Figure 11, Route B), acetylNAC is converted to acetyl-CoA prior to ATP production. These two routes cannot be distinguished by isotopic labelling, and studying them is only possible using cell-free extracts; one requires CoASH, while the other does not.
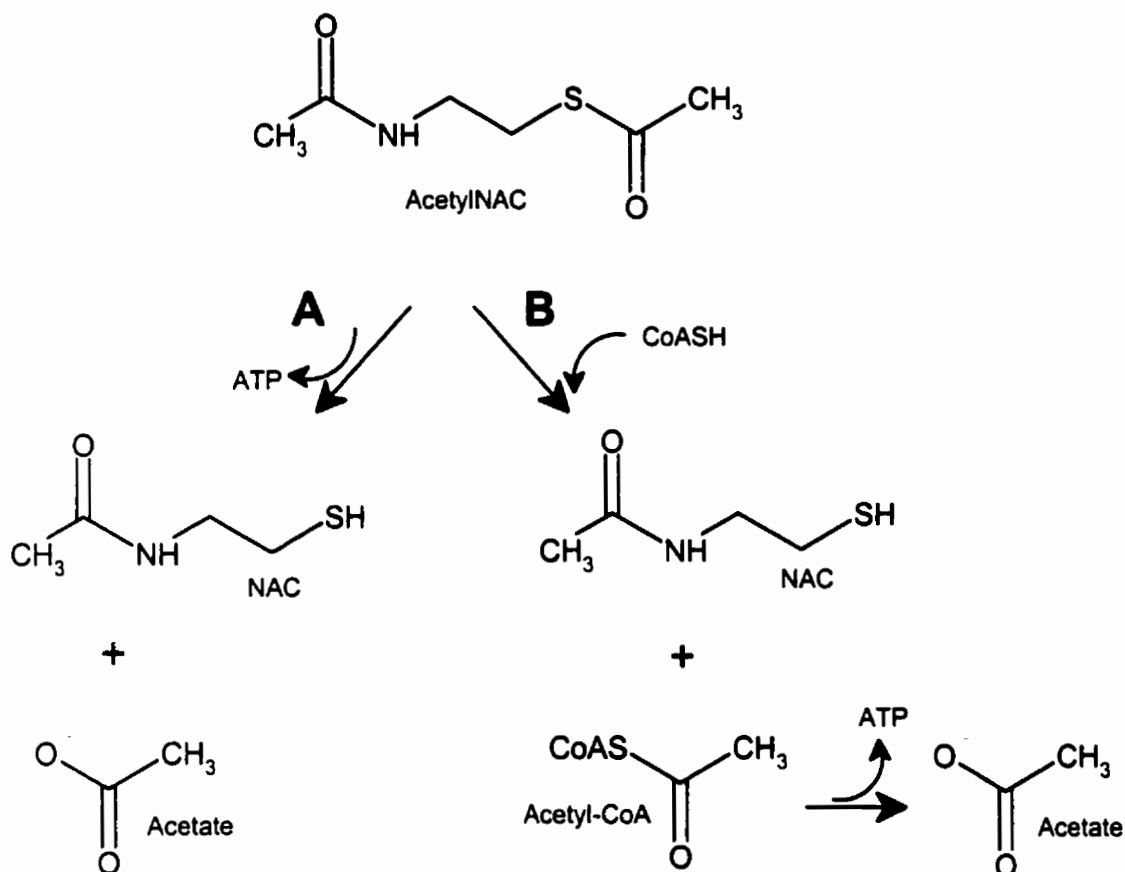
Figure 11. Proposed routes of metabolism of acetylNAC into acetate and NAC. (A) Direct usage of acetylNAC as a substrate for ATP production; (B) Conversion of acetylNAC to acetyl-CoA for ATP production.

The ability to assimilate NAC esters also raises the question as to whether NAC esters of four the acetate-butyrate pathway intermediates tested (Table 2) can also consumed. However, such esters are not commercially available.

Chapter 3: Butyrate Formation from [U-^{13}C]Amino Acids

The metabolism of amino acids into acetate and butyrate prompted further studies on the formation of butyrate from the amino acids glutamate, histidine, and lysine. In particular, the route of butyrate formation, be it directly from the amino acid as an intact four-carbon unit or from the combination of acetate derivatives, was determined.

3.1   Metabolic Interconversion of Acetate and Butyrate

Studying the formation of butyrate from an amino acid requires the use of universally ^{13}C-labelled substrates. The presence of four contiguous ^{13}C atoms, detectable by high-resolution ^{13}C-NMR spectroscopy, would indicate that butyrate is formed from the amino acid as an intact C_4 unit. It is therefore essential that any [^{13}C$_4$]butyrate produced accumulates as an end-product in detectable quantities. Yet, whether ^{13}C$_4$ labelled butyrate accumulates depends on the extent of its breakdown to acetate (Figure 8, Route C). The extent of the breakdown can be investigated during glutamate catabolism by including [1-^{13}C]butyrate in the *Fusobacterium* resuspensions.

F. nucleatum and *F. varium* were resuspended in PBS containing [1-^{13}C]butyrate and unlabelled L-glutamate. At the end of the incubation period, acetate and butyrate were isolated as 4-bromophenacyl esters, which were separated by silica gel chromatography and analyzed by ^{13}C-NMR spectroscopy.

The carboxyl carbons of acetate and butyrate and C-3 of butyrate exhibited ^{13}C enrichments (Table 4, Expts. 1 and 2). The lower ^{13}C enrichment in acetate indicated that only a small amount of the initial butyrate was broken into C$_2$ units. Moreover, the very small enrichment measured at C-3 of butyrate suggested that only a few of the labelled C$_2$ units recombined to form butyrate. These results demonstrate that although butyrate is not a dead-end product, its metabolic turnover is sufficiently slow so that the isotopic composition of butyrate reflects its route of formation (Figure 8).

Table 4. Distribution of ^{13}C in metabolic end-products after incubation with labelled substrates.

Expt.	Labelled Substrate (^{13}C %)	Organism	^{13}C Enrichment in 4-bromophenacyl esters [a]					
			Acetate		Butyrate			
			C-1	C-2	C-1	C-2	C-3	C-4
1	Sodium [1-^{13}C]-butyrate (40%) [b]	*F. nucleatum*	5.6	0.0	25.6	0.0	0.4	-0.1
2	Sodium [1-^{13}C]-butyrate (40%) [b]	*F. varium*	4.5	0.0	17.4	-0.2	1.3	-0.1
3	L-[1-^{13}C]Glutamic acid (10%) [c]	*F. nucleatum*	5.1	-0.1	8.5	-0.2	3.3	-0.2

[a] A standard deviation of 0.1 was calculated from the peak heights of the natural abundance signals contributed by the derivatization reagent
[b] Co-administered with unlabelled L-glutamate (10 mM)
[c] Co-administered with unlabelled sodium acetate (10 mM)

Since butyrate is not a dead-end product, the acetate-butyrate pathway (Figure 1) is not a one-way pathway from acetate to butyrate. The pathway

merely serves as a connection between acetate and butyrate, two end-products of amino acid catabolism that are in constant flux. This connection allows both the production and consumption of NADH.

Furthermore, the catabolism of L-[1-^{13}C]glutamate by *F. nucleatum* was examined to determine whether metabolism of the four-carbon intermediates between glutamate and butyrate would redistribute the single ^{13}C label. The acetate and butyrate end-products were ^{13}C-enriched at the carboxyl carbons and at C-3 of butyrate (Table 4, Expt. 3). The distribution of label over the three positions was similar to that obtained in the [1-^{13}C]butyrate experiments, suggesting that asymmetric labelling within glutamate is maintained to a significant extent on conversion to butyrate. Indeed, similar unequal distributions of label in butyrate produced from singly labelled samples of glutamate by *F. nucleatum* growing on peptone medium have been interpreted in terms of the hydroxyglutarate pathway[63] (Figure 4), which transfers four contiguous carbons of glutamate into butyrate.

An alternative route for the formation of butyrate from glutamate in anaerobic bacteria is provided by the methylaspartate pathway (Figure 3), in which acetate units formed from the catabolism of an amino acid are combined to generate butyrate; butyrate is not derived from glutamate as an intact C_4 unit. Acetate units derived from a [U-^{13}C] amino acid would be labelled at both carbon atoms and combination of these units would generate butyrate labelled in all carbons, the same isotopic distribution as that obtained when butyrate is derived

as an intact unit from a [U-^{13}C]amino acid. However, the addition of unlabelled C_2

units would reduce the formation of [^{13}C$_4$]butyrate by the combination of two

labelled units (Figure 8, Route C) more than the path that maintains an intact C_4

unit (Figure 8, Route A). A baseline for the formation of butyrate by combination

of acetate units was established by incubating resuspended cells with [1,2-

^{13}C$_2$]acetate and glutamate. The results (Table 5, Expts. 4 and 5) indicate similar

levels of ^{13}C$_2$ enrichments (6%) in acetate and butyrate. Degradation of

glutamate via the methylaspartate pathway in *F. varium* produces two acetates

that must be recombined to form butyrate, consistent with the nearly equal

enrichment levels in acetate and butyrate. The small ^{13}C$_4$ enrichment observed

can be explained from the statistical combination of two ^{13}C$_2$ acetate units.

Whereas, in *F. nucleatum* (Table 5, Expt. 6), an 8% ^{13}C$_2$ enrichment is

observed in acetate, compared to only 2.7% ^{13}C$_2$ enrichment in butyrate. The

lower enrichment in butyrate is consistent with the hydroxyglutarate pathway,

which forms unlabelled butyrate directly. The presence of ^{13}C$_2$ labelling must

arise from the combination of labelled acetate and unlabelled acetate derived

from glutamate.

From an energetics standpoint, in *F. varium*, where glutamate is degraded

by the methylaspartate pathway, NADH formed by the conversion of pyruvate to

acetyl-CoA is recycled by the synthesis of butyrate from acetate. All butyrate

formed must arise from acetate, giving an equal ^{13}C$_2$-enrichments of labelling in

acetate and butyrate.

**Table 5. Distribution of ^{13}C in metabolic
end-products after incubation with [$^{13}C_2$]acetate (20% ^{13}C).**

Expt.	Labelled Substrate	Organism	^{13}C Enrichment in 4-bromophenacyl esters [a]			
			Acetate	Butyrate		
			1,2-$^{13}C_2$	1,2-$^{13}C_2$	3,4-$^{13}C_2$	$^{13}C_4$
4	Sodium [1,2-$^{13}C_2$]-acetate [b]	*F. varium*	6.4	6.4	6.5	0.9
5	Sodium [1,2-$^{13}C_2$]-acetate [c]	*F. varium*	5.7	6.0	6.1	0.6
6	Sodium [1,2-$^{13}C_2$]-acetate [b]	*F. nucleatum*	7.8	2.7	2.8	0.4

[a]   A standard deviation of 0.1 was calculated from the peak heights of the
      natural abundance signals contributed by the derivatization reagent
[b]   Co-administered with unlabelled L-glutamate (10 mM)
[c]   Co-administered with unlabelled D-glutamate (10 mM)

In *F. nucleatum*, direct formation of crotonyl-CoA from glutamate via the

hydroxyglutarate pathway would decrease the need for acetate to be converted

to butyrate for NAD⁺ regeneration. The NADH generated on the conversion of

crotonyl-CoA to acetyl-CoA is recycled to NAD⁺ by the reduction of crotonyl-CoA

to butyrate. Thus, the direct conversion of unlabelled crotonyl-CoA to butyrate is

key to energy production from glutamate. As a result, less label is recovered in

butyrate.

In addition to $^{13}C_2$-labelled butyrate species, [$^{13}C_4$]butyrate was also

detected in three experiments (Table 5), indicating that the statistical combination

of two [$^{13}C_2$]acetate units is observable. Studying butyrate formation using

universally ^{13}C-labelled amino acids requires that any [^{13}C$_4$]butyrate derived as an intact unit be distinguishable from that produced by combination. The co-administration of unlabelled acetate with the U-^{13}C-labelled amino acids would be expected to minimize the [^{13}C$_4$]butyrate formed from combination; the amount of unlabelled acetate required needs to be established.

3.2   Catabolism of Universally ^{13}C-Labelled Amino Acids

To determine whether butyrate is formed from the amino acids glutamate, histidine, and lysine as an intact C$_4$ unit, *F. nucleatum* and *F. varium* resuspensions were incubated with [U-^{13}C]amino acids (Table 6).

For *F. nucleatum*, the 62.9 MHz proton decoupled ^{13}C-NMR spectrum of the 4-bromophenacyl butyrate sample isolated from the L-[^{13}C$_5$]glutamate resuspension in the presence of 10 mM acetate (Table 6, Expt 7) exhibited singlet signals for the carbon atoms supplied by the reagent and multiline resonances for each carbon atom in the butyrate moiety (Figure 12); three-line patterns for C-1 and C-4, seven lines for C-2, and five lines for C-3 were observed. Each group of lines exhibited a natural abundance resonance flanked by a higher intensity doublet due to coupling between C-1/C-2 and C-3/C-4 ($^1J_{C1C2}$ = 57.7 Hz and $^1J_{C3C4}$ = 34.8 Hz), indicating the intact incorporation of C$_2$ units formed from the amino acid. The four additional signals observed for C-2 were attributed to a doublet of doublets pattern due to simultaneous coupling of C-2 to C-1 and C-3 ($^1J_{C1C2}$ = 57.7 Hz and $^1J_{C3C4}$ = 33.9 Hz). A similar group of

signals would be expected at C-3, but only the outer lines of the doublet of doublets were distinct. The sum of $^1J_{C2C3}$ and $^1J_{C3C4}$ from the spacing of the outer lines at C-3 and $^1J_{C2C3}$ calculated from the C-2 signals indicated that the couplings between C-2/C-3 and C-3/C-4 were similar. Thus, the two inner lines of the doublet of doublets are close together and have chemical shifts that are similar to the natural abundance singlet. As a result, the central line in the five-line pattern at C-3 has a higher relative intensity than the central lines of the patterns associated with the other carbon atoms.

Table 6. Distribution of ^{13}C in metabolic end-products after incubation with [U-^{13}C]amino acids (10% ^{13}C).

Expt.	Labelled Substrate	Organism	^{13}C Enrichment in 4-bromophenacyl esters [a]			
			Acetate	Butyrate		
			1,2-^{13}C$_2$	1,2-^{13}C$_2$	3,4-^{13}C$_2$	^{13}C$_4$
7	L-[U-^{13}C$_5$]Glutamate [b]	*F. nucleatum*	5.4	4.2	4.8	3.2
8	L-[U-^{13}C$_5$]Glutamate [b]	*F. varium*	7.5	6.4	6.6	0.9
9	L-[U-^{13}C$_5$]Glutamate [c]	*F. nucleatum*	1.4	1.7	2.1	2.4
10	L-[U-^{13}C$_5$]Glutamate [c]	*F. varium*	2.1	1.8	1.9	nd
11	L-[U-^{13}C$_6$]Histidine [c]	*F. nucleatum*	1.5	1.4	1.8	2.3
12	L-[U-^{13}C$_6$]Histidine [c]	*F. varium*	1.3	0.5	0.5	nd
13	L-[U-^{13}C$_6$]Lysine [c]	*F. nucleatum*	nd	1.4	1.4	0.8
14	L-[U-^{13}C$_6$]Lysine [c]	*F. varium*	2.3	2.1	2.1	1.1

[a] A standard deviation of 0.1 was calculated from the peak heights of the natural abundance signals contributed by the derivatization reagent; nd = not detected
[b] Co-administered with unlabelled sodium acetate (10 mM)
[c] Co-administered with unlabelled sodium acetate (100 mM)

The doublet of doublet patterns observed for the C-2 and C-3 signals in the 62.9 MHz ^{13}C-NMR spectrum (Figure 12) indicates that each of these carbons has two ^{13}C neighbours. While the coupling of C-2 and C-3 to two other carbons is consistent with a ^{13}C$_4$ sample, it only demonstrates the presence of two ^{13}C$_3$ units. To demonstrate that the butyrate moiety contained four atoms of ^{13}C, the ^{13}C NMR spectrum of the same *F. nucleatum* derived butyrate ester (Table 6, Expt. 7) was acquired at 100.6 MHz and examined for long-range couplings between carbon atoms. The signals due to the carbons provided by the 4-bromophenacyl reagent appeared as singlets in the proton decoupled spectrum, whereas an eight-line pattern was now evident for each carbon atom in the butyrate moiety (Figure 13), demonstrating the coupling of each carbon atom to three others. The internal carbons had two large one-bond couplings as observed at 62.9 MHz and a smaller two-bond coupling, whereas the terminal carbons had one large coupling and two smaller couplings due to coupling over two and three bonds. These coupling patterns are only consistent with the presence of four contiguous atoms of ^{13}C in butyrate. Thus, the ^{13}C-labelling results indicate that the butyrate sample derived from L-[^{13}C$_5$]glutamate is a mixture of ^{13}C$_4$ and two ^{13}C$_2$ (C-1/C-2 and C-3/C-4) enriched species and a species containing ^{13}C only at natural abundance.

Figure 12. ^{13}C-NMR spectrum at 62.9 MHz of the 4-bromophenacyl butyrate isolated from the catabolism of L-[U-^{13}C$_5$]glutamate by *F. nucleatum* in the presence of 10 mM acetate. (Table 6, Expt. 7). The signals representing the butyrate moiety are shown.

On the contrary, the 62.9 MHz ^{13}C-NMR spectrum of the 4-bromophenacyl butyrate isolated from the catabolism of L-[^{13}C$_5$]glutamate in the presence of 10 mM acetate by *F. varium* (Table 6, Expt. 8) exhibited natural abundance singlet signals flanked by doublets at all four carbons in the butyrate moiety and only a minor set of doublets of doublets at C-2 and C-3 (Figure 14). The small set of doublets of doublets indicates that the 4-bromophenacyl butyrate sample consists of unlabelled butyrate, [1,2-^{13}C$_2$]butyrate, [3,4-^{13}C$_2$]butyrate, and an almost undetectable amount of ^{13}C$_4$-butyrate. The small amount of ^{13}C$_4$-butyrate present can be explained statistically by the combination of two ^{13}C$_2$ acetate units.
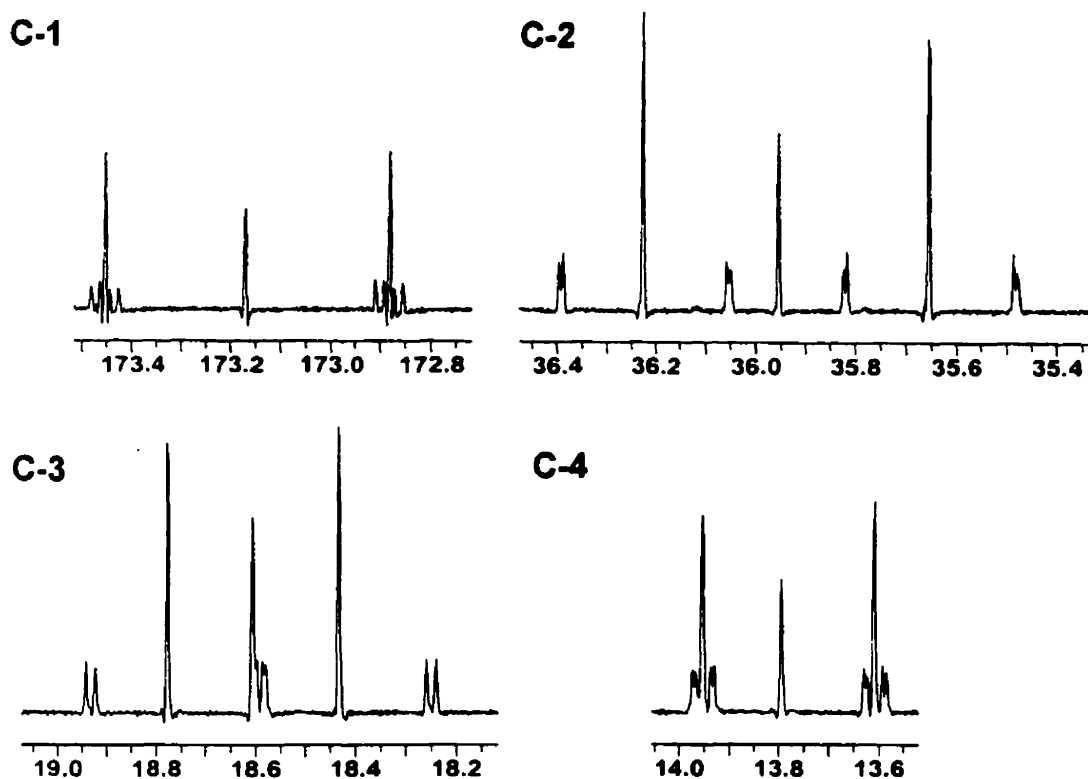
Figure 13. ^{13}C-NMR spectrum at 100.6 MHz of the 4-bromophenacyl butyrate isolated from the catabolism of L-[U-^{13}C$_5$]glutamate by *F. nucleatum* in the presence of 10 mM acetate (Table 6, Expt. 7). The signals representing the butyrate moiety are shown.
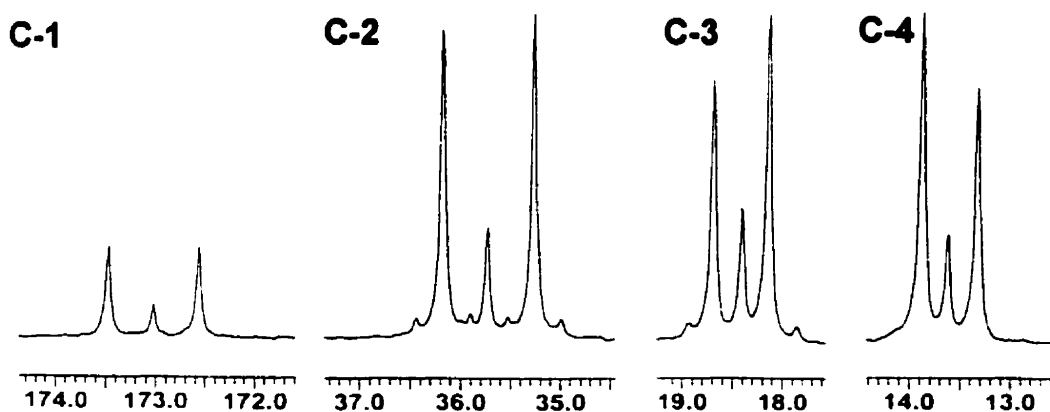
Figure 14. ^{13}C-NMR spectrum at 62.9 MHz of the 4-bromophenacyl butyrate isolated from the catabolism of L-[U-^{13}C$_5$]glutamate by *F. varium* in the presence of 10 mM acetate (Table 6, Expt. 8). The signals representing the butyrate moiety are shown.

To distinguish between the $^{13}C_4$ butyrate formed statistically by the combination of labelled acetate units and by that formed intact from the amino acid substrate, the L-[$^{13}C_5$]glutamate experiments were repeated using a higher concentration of unlabelled acetate (100 mM, Table 6, Expts. 9 and 10). The dilution of $^{13}C_2$ species in the acetate pool was indicated by much lower relative intensities of the doublet signals in the ^{13}C-NMR spectra of the 4-bromophenacyl derivatives of acetate and butyrate. In the *F. nucleatum* generated sample, the relative amount of the $^{13}C_4$ butyrate species was decreased by only a small extent by increasing the concentration of unlabeled acetate (Figure 15). The coupling constants for the atoms of the butyrate moiety were determined (Hz; J_{C1C2} 57.6, J_{C1C3} 1.8, J_{C1C4} 3.8, J_{C2C3} 34.0, J_{C2C4} 0.8, J_{C3C4} 34.7). By contrast, signals due to C-2/C-3 coupling were no longer observed in the *F. varium* sample of butyrate (Figure 16).
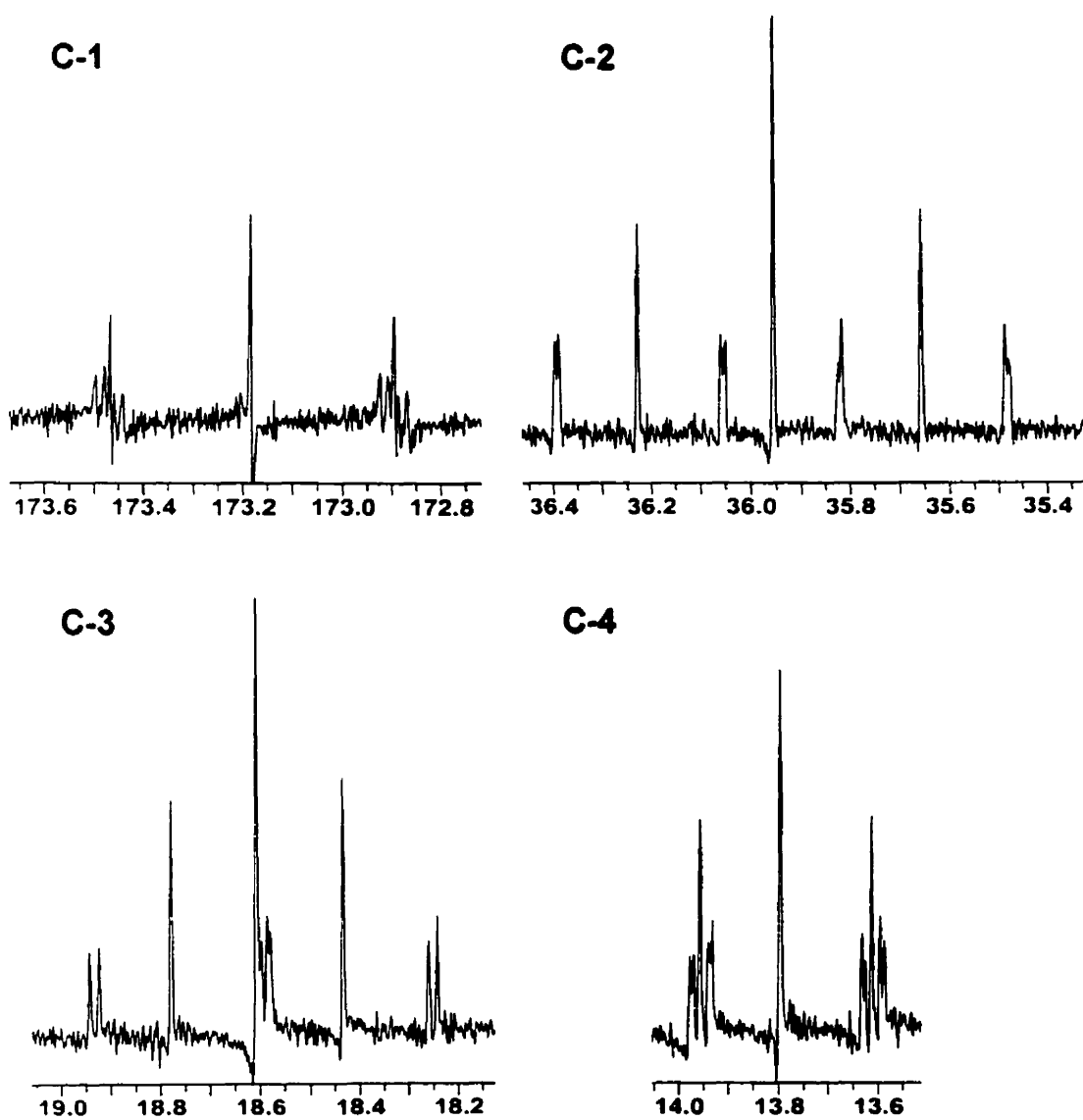
Figure 15. ^{13}C-NMR spectrum at 100.6 MHz of the 4-bromophenacyl butyrate isolated from the catabolism of L-[U-^{13}C$_5$]glutamate by *F. nucleatum* in the presence of 100 mM acetate (Table 6, Expt. 9). The signals representing the butyrate moiety are shown.
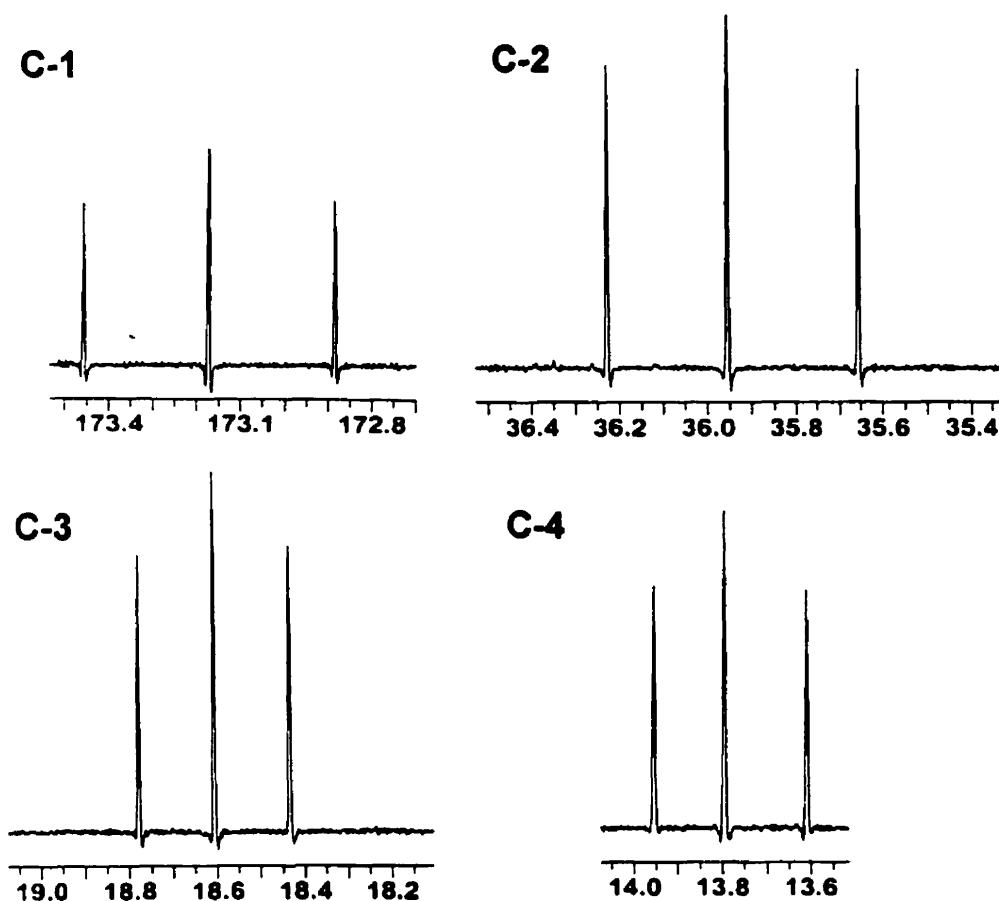
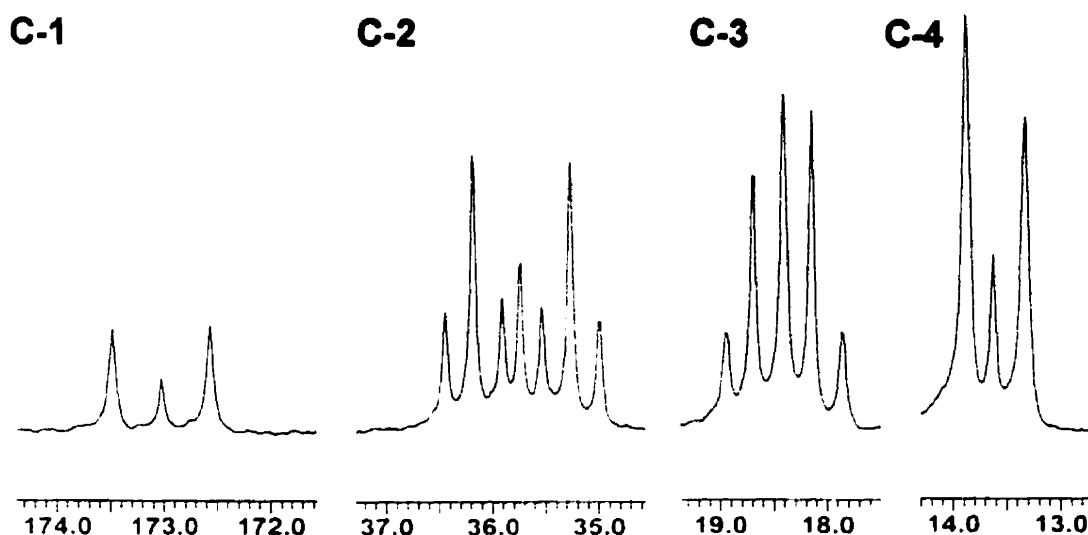Figure 16. ^{13}C-NMR spectrum at 100.6 MHz of the 4-bromophenacyl butyrate isolated from the catabolism of L-[U-^{13}C$_5$]glutamate by *F. varium* in the presence of 100 mM acetate (Table 6, Expt. 10). The signals representing the butyrate moiety are shown.

These results demonstrate that butyrate is indeed formed from glutamate as an intact C$_4$ unit in *F. nucleatum*, via the hydroxyglutarate pathway (Figure 4). Similarly, the degradation of glutamate by the methylaspartate pathway in *F. varium* is supported (Figure 3).

Having established that 100 mM acetate was sufficient to distinguish between butyrate formation as an intact unit and by recombination of acetate units, the catabolism of histidine and lysine to butyrate was investigated (Table 6, Expts. 11-14). The level of ^{13}C enrichment in the 4-bromophenacyl esters formed by degradation of histidine was similar to those in the comparable glutamate experiment in F. nucleatum, but somewhat lower in the F. varium samples. However, the coupling patterns at 100.6 MHz were identical with the glutamate-derived butyrate samples, demonstrating that butyrate is derived from histidine as an intact unit in F. nucleatum, but not in F. varium. These similarities observed with both glutamate and histidine support the theory that histidine is degraded to glutamate (Figure 5).[28]

The relative amount of the ^{13}C$_4$ species in the lysine experiments was less than the ^{13}C$_2$ species, and only about one-third of the levels obtained in the glutamate and histidine experiments in F. nucleatum. Nevertheless, two- and three-bond couplings were present in the butyrate samples derived from lysine in both organisms, indicating the formation of butyrate from lysine as an intact unit. Experiments to determine the position of cleavage in the lysine backbone are described in the next chapter.

In addition, no ^{13}C$_2$[acetate] was detected in the lysine experiment with F. nucleatum (Table 6, Expt. 13). The ability to detect labelled acetate requires that any labelled acetate formed within the cell exits into the resuspension. With a high external concentration of acetate (100 mM), such a process is

thermodynamically disfavoured; however, this phenomenon is not a very valid explanation, as labelled acetate was detected in the other experiments involving 100 mM acetate. The only other possible explanation relates to the usage of acetate by the cells: if the cells are in a growing state, acetate derivatives would be consumed in the biosynthesis of fatty acids and other carbon compounds.

In summary, the butyrate formed by the amino acid glutamate, histidine, and lysine originate from either C_2 or C_4 intermediates from the amino acids. That is, common themes are present in the amino acid degradation pathways. These intermediates reiterate the importance of the acetate-butyrate pathway (Figure 1) in the metabolism of the two *Fusobacterium* species studied. Without this pathway, or one that is fully functional, amino acid catabolism, and hence growth and cellular reproduction, would cease to occur. This pathway is analogous to the central citric acid cycle found in other organisms, including humans.

Since the acetate-butyrate pathway is a central and essential metabolic pathway, it is an ideal candidate for targeting by antibiotics. Certainly, the inhibition of the enzymes in the pathway would disrupt cellular metabolism. When designing a synthetic antibiotic, the details of the target enzyme must be clearly known, meaning that the enzymes must be purified and well-characterized. The only caveat, however, is that the enzymes in the acetate-butyrate pathway resembles those in the fatty acid biosynthesis pathway of advanced organisms. As such, the designed antibiotic must target only the intended enzymes.

Chapter 4: Lysine Analysis and Catabolism

4.1 Rationale For Using $^{13}C_2$-Labelled Lysine

The retention of an intact C_4 unit in the catabolism of L-lysine to butyrate by *F. nucleatum* and *F. varium* suggests that the C_6 lysine molecule must be cleaved into distinctive C_2 and C_4 units, which can lead directly to acetate and butyrate, respectively. In order to produce both C_2 and C_4 units, lysine must be cleaved between either atoms C-2 and C-3 or C-4 and C-5. These two possible bond cleavage locations were studied using L-[2,3-$^{13}C_2$]- and L-[4,5-$^{13}C_2$]lysine, provided by Ross Witherell.[92] D-Lysine samples with the same $^{13}C_2$ labelling patterns were also provided to aid in the identification of the possibly separate pathways for the two lysine stereoisomers.

The proposed pathway of L-lysine catabolism in *Clostridium* species (Figure 6) suggests that butyrate is derived from C-3 to C-6 of the L-lysine backbone, while butyrate from D-lysine is derived from C-1 to C-4 (Figure 7). As discussed in Chapter 1, the two pathways of lysine catabolism in *F. nucleatum* have been suggested to be similar to those proposed for *Clostridium*, but the available isotopic and enzymatic evidence is ambiguous. However, the two possible cleavage sites can be correctly and unambiguously distinguished using D- and L-lysine labelled with $^{13}C_2$ at the C-2/C-3 and C-4/C-5 positions. The positions of the two ^{13}C labels were chosen because they are connected by a bond that is retained in one pathway and cleaved in the other pathway. Bond

cleavage or retention can be observed by the absence or presence, respectively, of ^{13}C-^{13}C coupling in the NMR spectra of the isolated 4-bromophenacyl butyrate esters. Only a coupled $^{13}C_2$ unit indicates that bond cleavage has not occurred.

The potential presence of a lysine racemase in *F. nucleatum* or *F. varium* can complicate the interpretation of results by catalyzing the interconversion of the D- and L-isomers. The possible incorporations of a coupled $^{13}C_2$ unit from lysine into butyrate are summarized in Table 7, and even with a racemase, a unique pattern of the retention of coupling from the four labelled lysine samples arises from each possible route or combination of routes of lysine catabolism.

Table 7. Possible incorporations of a coupled $^{13}C_2$ unit from lysine into butyrate by L- and D-lysine pathways (Figure 6 and 7).

Labelled Lysine	Separate D- and L- Pathways (Case #1)	L-Pathway and Racemase (Case #2)	D-Pathway and Racemase (Case #3)	Separate D- and L-Pathways and Racemase (Case #4)
D-[2,3-$^{13}C_2$]	✓	X	✓	✓
L-[2,3-$^{13}C_2$]	X	X	✓	✓
D-[4,5-$^{13}C_2$]	X	✓	X	✓
L-[4,5-$^{13}C_2$]	✓	✓	X	✓

✓ Intact incorporation of a coupled $^{13}C_2$ unit
X No intact incorporation of a coupled $^{13}C_2$ unit

4.2 Isotopic and Enantiomeric Analysis of $^{13}C_2$ Lysine Samples

The successful application of this approach requires specially labelled and enantiomerically pure lysine samples. However, ^{1}H-NMR spectroscopy indicated that the provided [$^{13}C_2$]lysine samples were significantly less than the 99% $^{13}C_2$ enrichment expected,[92] and a rigorous analysis was required before the samples could be used for the study of lysine catabolism.

The lysine samples were analyzed by cation electrospray MS for isotopic enrichment and by reversed-phased HPLC[93,94] using a triethylammonium phosphate buffer system for enantiomeric purity (Table 8). For enantiomeric analysis, samples were derivatized with FDA reagent, and the disubstituted diastereomers (Figure 17) were separated by HPLC. Both of the $^{13}C_2$-labelled L-lysine samples were determined to be virtually enantiomerically pure (94-98% L). The D-lysine samples, however, were roughly racemic mixtures. Sample HPLC chromatograms for the analysis of L-[4,5-$^{13}C_2$]- and D-[4,5-$^{13}C_2$]lysine are shown in Figure 18.

Table 8. Summary of D- and L-[2,3-$^{13}C_2$]lysine and [4,5-$^{13}C_2$]lysine analysis.

Lysine Sample	% $^{13}C_2$ [a]	% D-isomer [b]	% L-isomer [b]
L-[2,3-$^{13}C_2$]lysine	64.3	2.4	97.6
L-[4,5-$^{13}C_2$]lysine	71.8	5.9	94.1
D-[2,3-$^{13}C_2$]lysine	54.5	46.9	53.1
D-[4,5-$^{13}C_2$]lysine	67.4	55.2	44.8

[a] Determined by MS; details provided in Table 9
[b] Determined by HPLC; average of duplicate injections
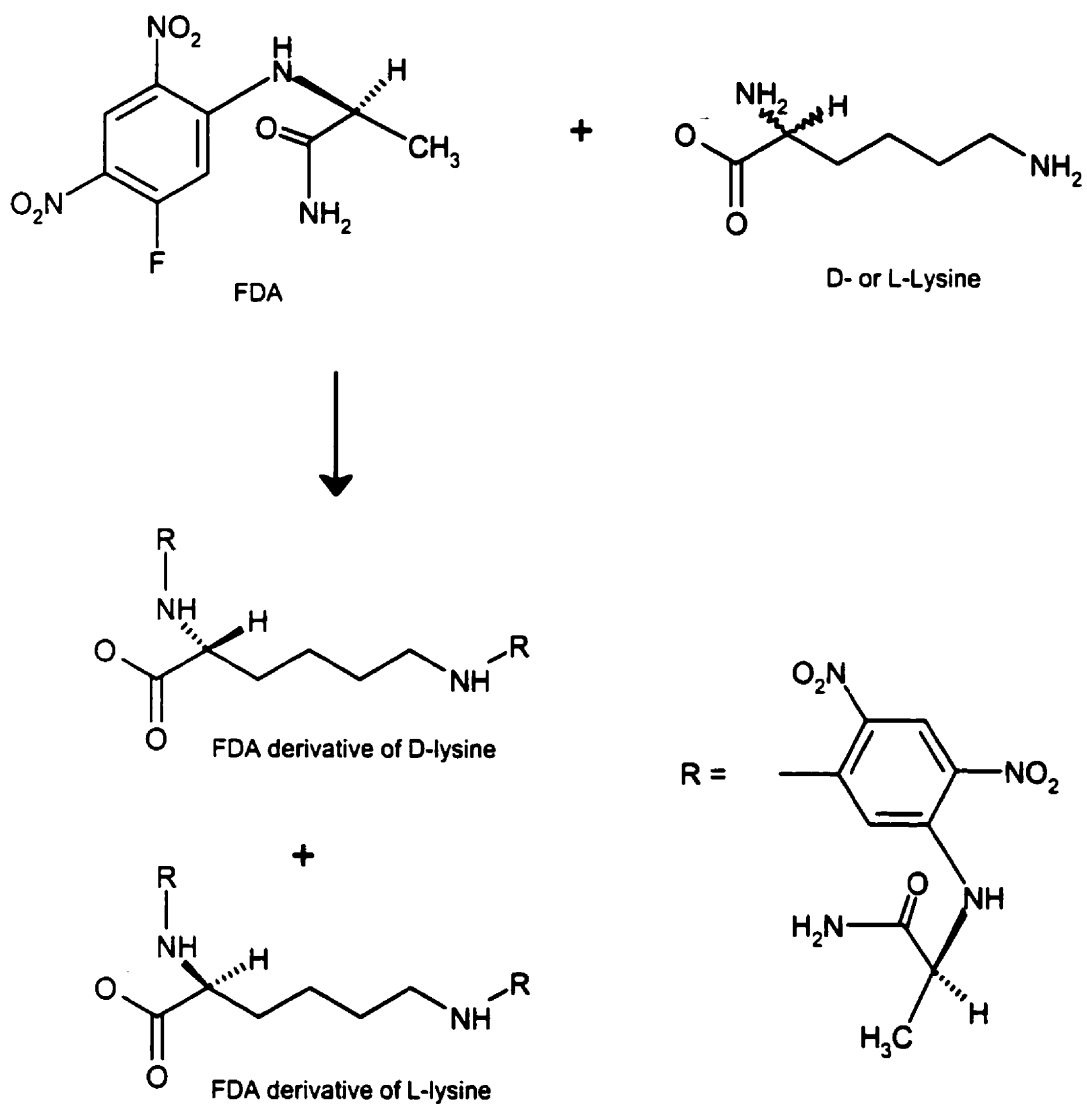
Figure 17. Derivatization of lysine with FDA reagent. Lysine enantiomers are converted to disubstituted diastereomeric derivatives that can be separated by HPLC.
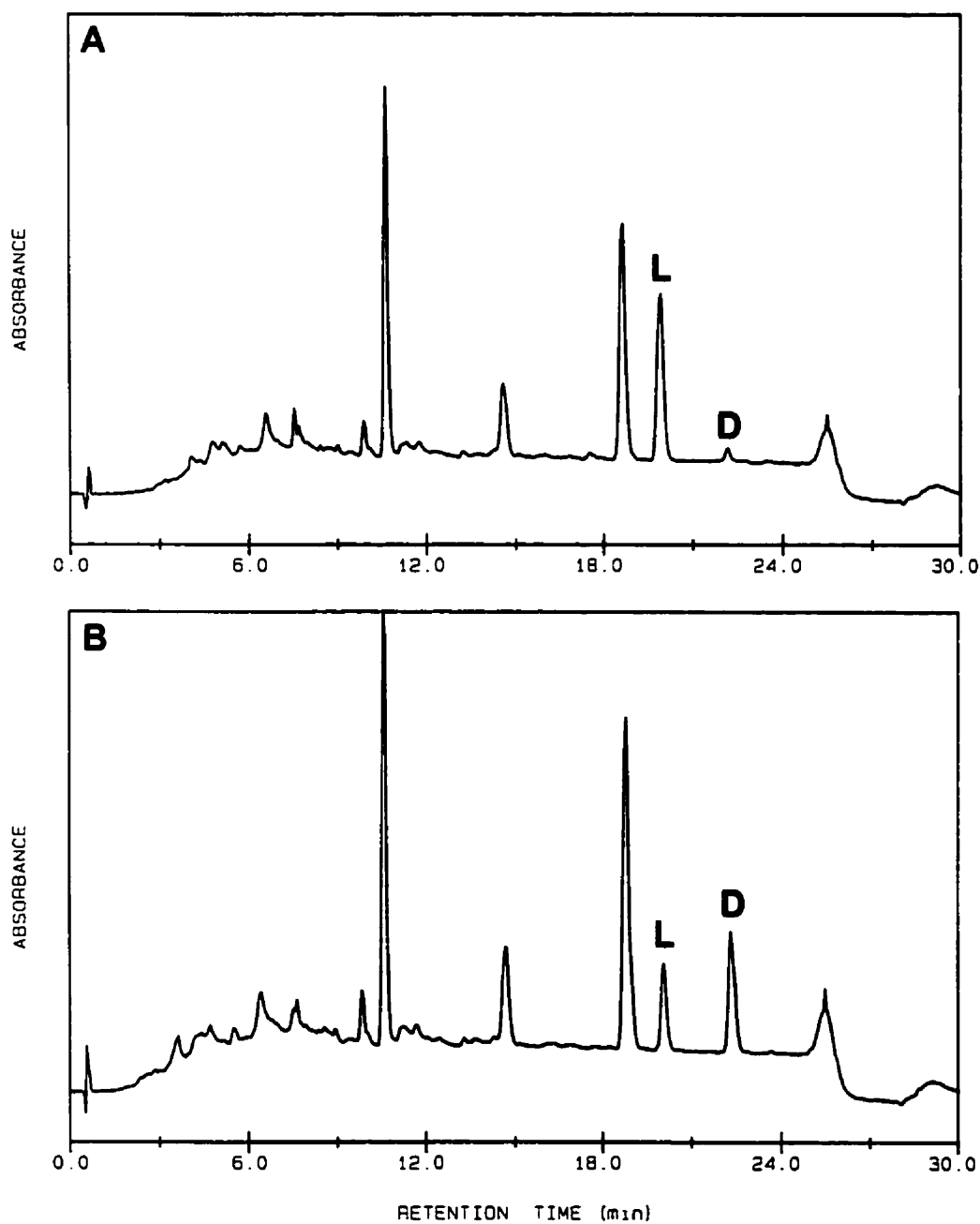
Figure 18. HPLC analysis of $^{13}C_2$-labelled lysine. (A) L-[4,5-$^{13}C_2$]- and (B) D-[4,5-$^{13}C_2$]lysine. Peaks corresponding to the elution of the FDA derivatives of L- and D-lysine are marked L and D, respectively. The mobile phase consisted of a gradient formed between triethylammonium phosphate (50mM, pH 3) and acetonitrile:2-propanol (4:1).

For the determination of $^{13}C_2$ enrichment by MS, the four labelled samples along with a natural abundance L-lysine sample were dissolved in water and analyzed by cation electrospray MS. A natural abundance D-lysine free base sample was not available, but in principal, its MS behaviour should be identical to that of L-lysine. Parent ions were revealed at m/z = 147, 148, and 149 for the natural abundance samples, while the labelled samples exhibited increased peak intensities at m/z = 149. Portions of the mass spectra depicting the parent ions are presented in Figure 19, while the information used for the calculation of isotopic enrichments is provided in Table 9.
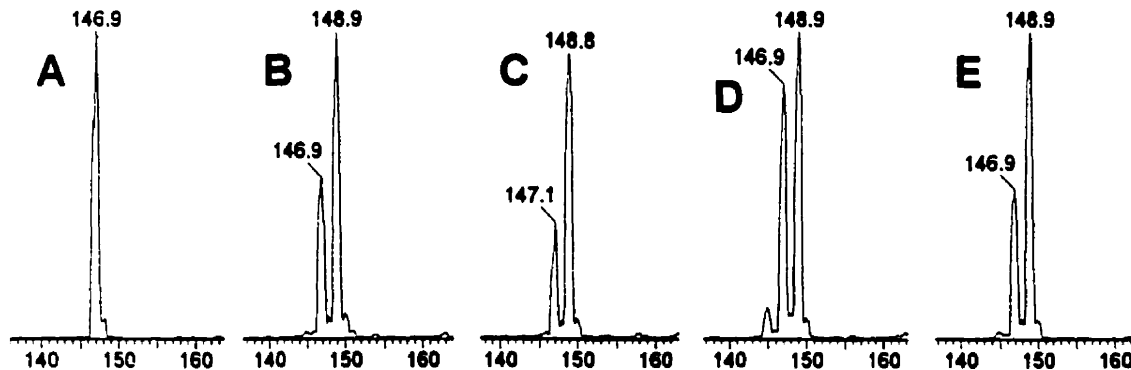
Figure 19. MS analysis of $^{13}C_2$-labelled lysine. (A) Natural abundance L-lysine, (B) L-[2,3-$^{13}C_2$]lysine, (C) L-[4,5-$^{13}C_2$]lysine, (D) D-[2,3-$^{13}C_2$]lysine, and (D) D-[4,5-$^{13}C_2$]lysine. The portions of the mass spectra representing the parent ions are shown.

Table 9. MS determination of the $^{13}C_2$ enrichments of $^{13}C_2$-labelled lysine.

Lysine Sample	Relative Base Peak Intensities [a]			% $^{13}C_2$ Enrichment
	m/z = 147	m/z = 148	m/z = 149	
Natural abundance L-lysine	100	7.80	1.05	--
L-[2,3-$^{13}C_2$]lysine	54.72	7.04	100	$\dfrac{100 - (54.72x0.0105)}{100 + 54.72} x100 = 64.3$
L-[4,5-$^{13}C_2$]lysine	38.77	6.92	100	$\dfrac{100 - (38.77x0.0105)}{100 + 38.77} x100 = 71.8$
D-[2,3-$^{13}C_2$]lysine	81.86	8.22	100	$\dfrac{100 - (81.86x0.0105)}{100 + 81.86} x100 = 54.5$
D-[4,5-$^{13}C_2$]lysine	47.68	5.83	100	$\dfrac{100 - (47.68x0.0105)}{100 + 47.68} x100 = 67.4$

[a] Average of two injections

The L-lysine samples were essentially enantiomerically pure and were determined to be approximately 64-72% $^{13}C_2$ enriched, suggesting that the $^{13}C_2$ labelling must exist in the L-isomers of the L-lysine samples. An explanation for the low level of $^{13}C_2$ observed is only up to speculation. Regardless, these L-lysine samples are suitable for feeding experiments.

On the other hand, the provided D-lysine samples were essentially racemic mixtures, with 47% and 55% D-lysine, and $^{13}C_2$ enrichments of 55% and 67%, respectively. Clearly, there is more $^{13}C_2$ labelling available than the amount of D-isomers. Even if the enrichments of the D-isomers in the samples are 100%, there is still excess $^{13}C_2$, indicating that some of the L-isomers are also labelled.

Conversely, the L-isomers may be 100% labelled, while the D-isomers contain less labelling. Of course, in-between situations involving all combinations are also possible. Due to these complications, further analysis to determine the amount of $^{13}C_2$ in each isomer is essential.

4.2.1 Detailed Analysis of D-[2,3-$^{13}C_2$]- and D-[4,5-$^{13}C_2$]Lysine Samples

The analysis of a single enantiomer in a racemic mixture is not an uncomplicated procedure. The determined method of choice for the analysis involved derivatizing the samples with FDA reagent, separating the diastereomers by HPLC, collecting the corresponding peaks, removing most of the buffer components by column chromatography, followed by analysis of the separated diastereomers by anion electrospray MS. The triethylammonium phosphate HPLC buffer previously used for enantiomeric analysis was replaced with ammonium acetate-fluoroacetate, which is more compatible with MS due to its higher volatility. In fact, the change of buffer system resulted in cleaner HPLC chromatograms with a more stable baseline and an improved peak separation between the two diastereomers (Figure 18 and Figure 20).

Prior to analyzing the $^{13}C_2$-labelled D-lysine samples, the protocol was evaluated using a natural abundance, racemic lysine sample to show that the proper derivatives could be isolated. The sample was derivatized with FDA, and the diasteromers were separated on a larger scale by HPLC, cleaned by column chromatography, and analyzed by MS. Both of the D- and L-lysine derivatives

revealed parent ions at m/z = 649 (Figure 21). The presence of m/z = 649 ions not only shows that the protocol is adequate, but also that the peaks collected from the HPLC chromatograms were indeed the correct FDA-derivatized products (Figure 17). Isotopic enrichments were calculated from the m/z = 649 and m/z = 651 peak intensities (Table 11). MS analysis was required, as ^{1}H-NMR spectroscopy proved unsuccessful in determining the complex structure of the isolated derivatives; the combination of insufficient spectroscopic resolution and a large amount of aqueous buffer components relative to the small amount of sample did not produce interpretable spectra.

Knowing that the procedure for separating and analyzing the diastereomers is able to the provide molecular masses of the FDA derivatives, the two $^{13}C_2$-labelled D-lysine samples were derivatized and separated by HPLC for MS analysis. The separated diastereomers, pooled from many HPLC injections, were re-analyzed by HPLC to determine the efficiency of the separation process. A summary of the analyses is provided in Table 10. The separation procedures via HPLC were over 98% efficient, indicating that the collected peaks were sufficiently enantiomerically pure for MS analysis. HPLC chromatograms of the separated FDA-derivatives are shown in Figure 20.

Table 10. Summary of rigorous D-[2,3-^{13}C$_2$]- and D-[4,5-^{13}C$_2$]lysine analysis.

Lysine Sample	Separated FDA Derivative of L-Lysine		Separated FDA Derivative of D-Lysine	
	% ^{13}C$_2$ [a]	% L-isomer [b]	% ^{13}C$_2$ [a]	% D-isomer [b]
D-[2,3-^{13}C$_2$]Lysine	12.0	> 98	96.6	> 99
D-[4,5-^{13}C$_2$]Lysine	23.6	> 99	94.9	> 98

[a] Determined by MS; details provided in Table 11
[b] Determined by HPLC

The enantiomerically pure FDA derivatives were analyzed by MS for the presence of m/z = 651, corresponding to ^{13}C$_2$-enriched species. The ^{13}C$_2$ enrichments determined for the D-[2,3-^{13}C$_2$]- and D-[4,5-^{13}C$_2$]lysine samples (Table 10) were calculated by comparing the relative ion peak intensities of m/z = 651 to the intensities of m/z = 649, corresponding to the unlabelled species. The isotopic contribution of m/z = 649 to m/z = 651 was subtracted from the intensities of the m/z = 651 peak to provide an accurate determination of ^{13}C$_2$ enrichments. Details are provided in Table 11, and relevant portions of the mass spectra are depicted in Figure 21. Enrichments calculated from the mass spectra of the separated derivatives correlate very well with the data provided in Table 8; that is, the amount of each lysine enantiomer and its corresponding enrichment correlate with the total enrichment measured in underivatized lysine. For D-[2,3-^{13}C$_2$]lysine, the calculated value of (46.9 x 0.966 + 53.1 x 0.120) = 51.7% is comparable to 54.5%. Similarly, for D-[4,5-^{13}C$_2$]lysine, the calculated value of (55.2 x 0.949 + 44.8 x 0.236) = 63.0 is close to 67.4%.
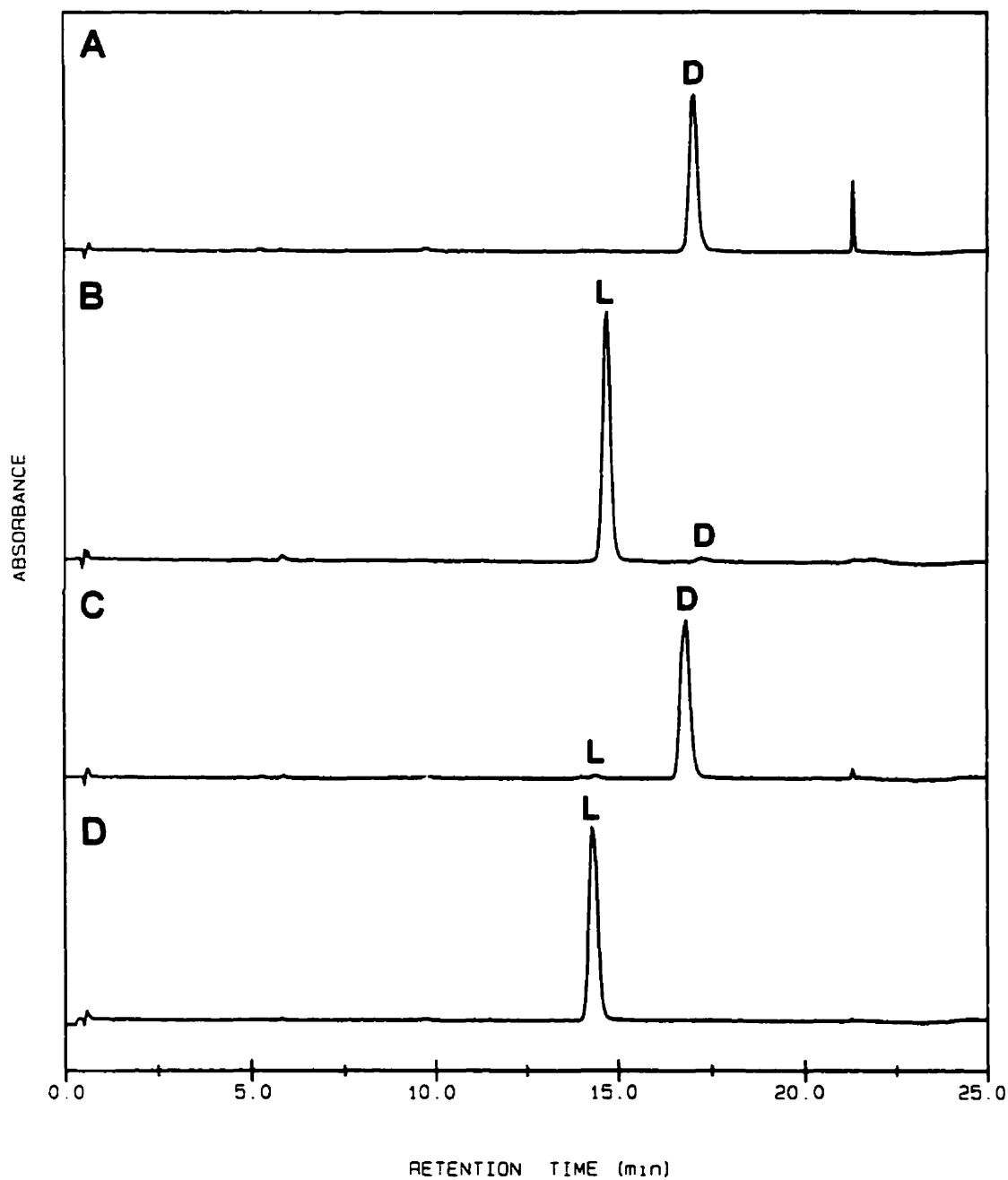
Figure 20. HPLC analysis of the separated FDA lysine derivatives. (A) FDA-D-lysine and (B) FDA-L-lysine from D-[2,3-^{13}C$_2$]lysine. (C) FDA-D-lysine and (D) FDA-L-lysine from D-[4,5-^{13}C$_2$]lysine. Peaks corresponding to the elution of the FDA derivatives of L- and D-lysine are marked L and D, respectively. The mobile phase consisted of a gradient formed between ammonium acetate-trifluoroacetate (100mM, pH 3) and acetonitrile:2-propanol (4:1).
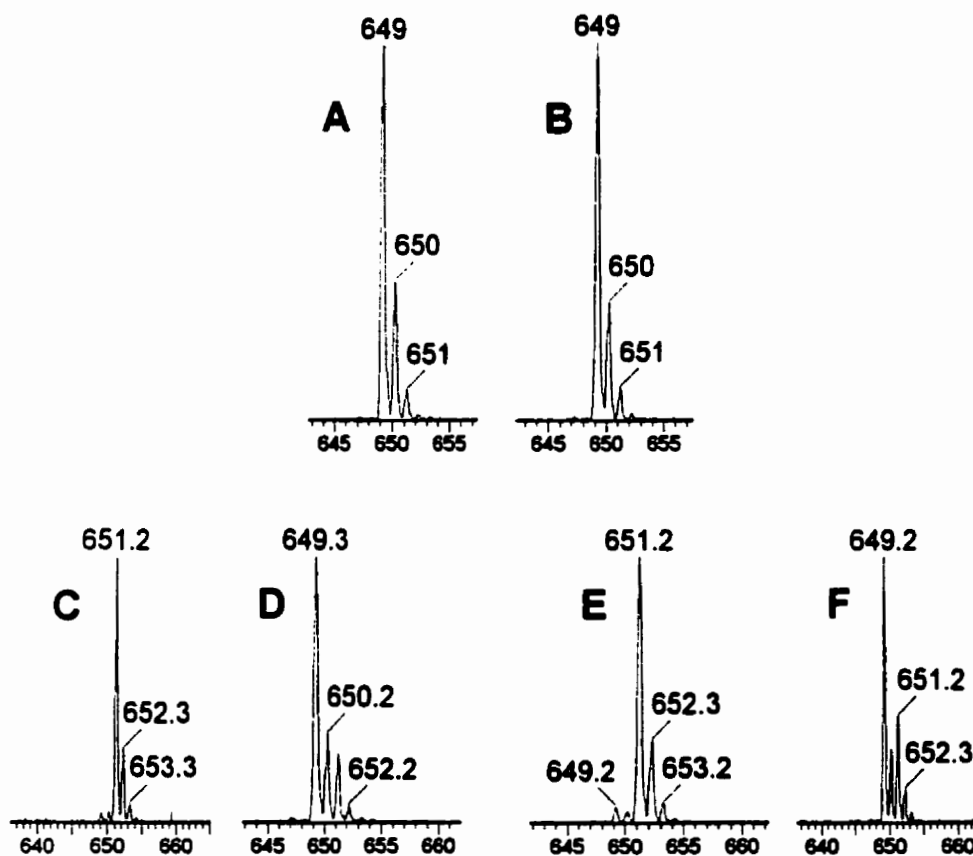
Figure 21. MS analysis of the separated FDA lysine derivatives. Natural abundance (A) D-lysine and (B) L-lysine. (C) D-Lysine and (D) L-lysine from D-[2,3-^{13}C$_2$]lysine. (E) D-Lysine and (F) L-lysine from D-[4,5-^{13}C$_2$]lysine. No fragmentation was observed under the conditions used.

Unfortunately, the presence of ^{13}C$_2$ enrichment in the large amounts of L-lysine in the D-[2,3-^{13}C$_2$]- and D-[4,5-^{13}C$_2$]lysine samples renders them unsuitable for use in feeding experiments, as it would defeat the original intentions of using specifically labelled and enantiomerically pure lysine. Only L-[2,3-^{13}C$_2$]- and L-[4,5-^{13}C$_2$]lysine are sufficiently pure for studying lysine catabolism.

<div align="center">

**Table 11. MS determination of $^{13}C_2$ enrichments in
the separated FDA derivatives of D-[2,3-$^{13}C_2$]- and D-[4,5-$^{13}C_2$]lysine.**

</div>

FDA derivative	Relative Base Peak Intensities [a]			% $^{13}C_2$ Enrichment
	$m/z = 649$	$m/z = 650$	$m/z = 651$	
Natural abundance L-lysine	100	32.9	7.93	--
L-lysine from D-[2,3-$^{13}C_2$]lysine	100	30.5	22.7	$\dfrac{22.7-7.93}{100+22.7} \times 100 = 12.0$
L-lysine from D-[4,5-$^{13}C_2$]lysine	100	31.1	41.2	$\dfrac{41.2-7.93}{100+41.2} \times 100 = 23.6$
Natural abundance D-lysine	100	35.2	8.13	--
D-lysine from D-[2,3-$^{13}C_2$]lysine	3.29	nd	100	$\dfrac{100-(3.29 \times 0.0813)}{100+3.29} \times 100 = 96.6$
D-lysine from D-[4,5-$^{13}C_2$]lysine	4.90	nd	100	$\dfrac{100-(4.90 \times 0.0813)}{100+4.90} \times 100 = 94.9$

[a] Average of two sets of scans; nd = not detected

4.3 Catabolism of L-[2,3-$^{13}C_2$]- and L-[4,5-$^{13}C_2$]Lysine

For feeding experiments, the level of $^{13}C_2$ enrichment (65-72%) in the L-lysine samples is above the level required. It is crucial to minimize the level of enrichment in the feeding experiments such that the odds of the recombination of labelled acetate units to form butyrate are minimized, but the enrichment must also be maintained at detectable levels. Enrichments of 10-15% $^{13}C_2$ are acceptable, considering that the [U-$^{13}C_6$]lysine experiments were performed at 10% $^{13}C_6$ enrichment; i.e. three times the total amount of ^{13}C. That is,

enrichments of 10-15% $^{13}C_2$ will have a smaller probability of labelled acetate recombination than enrichments of 10% $^{13}C_6$.

To obtain samples at a desired 10-15% $^{13}C_2$ enrichment, the labelled L-lysine samples were converted to their dihydrochloride salts and diluted with unlabelled L-lysine dihidrochloride; exact enrichments were determined by ^{13}C-NMR spectroscopy (Table 12). Feeding experiments involving the isotopically diluted samples were performed with *F. nucleatum* and *F. varium* (Table 12), and the end products were isolated as the 4-bromophenacyl esters of acetate and butyrate.

Table 12. Distribution of ^{13}C in metabolic end-products after incubation of *F. nucleatum* and *F. varium* with L-[2,3-$^{13}C_2$]- and L-[4,5-$^{13}C_2$]lysine.

Expt.	Lysine [b] (% $^{13}C_2$)	Organism	^{13}C Enrichments in 4-bromophenacyl esters [a]						
			^{13}C Acetate		^{13}C Butyrate				[2,3-$^{13}C_2$]- Butyrate
			C-1	C-2	C-1	C-2	C-3	C-4	
15	L-[4,5-$^{13}C_2$] (14.7)	*F. nucleatum*	3.2	3.1	0.6	1.4	1.3	1.0	5.4
16	L-[4,5-$^{13}C_2$] (12.9)	*F. varium*	2.8	2.8	1.8	2.4	2.2	2.0	0.9
17	L-[2,3-$^{13}C_2$] (14.8)	*F. nucleatum*	2.6	2.3	4.7	3.0	1.6	1.9	0.4
18	L-[2,3-$^{13}C_2$] (13.7)	*F. varium*	2.6	2.9	3.5	2.9	2.0	2.1	0.4

[a] A standard deviation of 0.1 was calculated from the peak heights of the natural abundance signals contributed by the derivatization reagent
[b] Lysine (10 mM) was co-administered with unlabelled sodium acetate (10 mM)

By incubating $^{13}C_2$-labelled L-lysine with *Fusobacterium* resuspensions and isolating the end-products as the 4-bromophenacyl esters of acetate and butyrate, it was possible to deduce the site of bond cleavage in L-lysine. Bond retention is indicated by the presence of ^{13}C-^{13}C coupling, whereas bond cleavage results in a loss of the coupling. After L-[4,5-$^{13}C_2$]lysine was administered to *F. nucleatum* (Table 12, Expt. 15), 4-bromophenacyl butyrate was isolated and analyzed by ^{13}C-NMR spectroscopy, revealing a 2,3-$^{13}C_2$ labelling pattern (J_{C2C3} = 34.0 Hz) in the butyrate moiety. The $^{13}C_2$ enrichment of 5.4% clearly suggests that butyrate is derived from C-3 to C-6 of L-lysine and that bond cleavage occured between C-2 and C-3 (Figure 6). Smaller incorporations of single ^{13}C label into each carbon of butyrate were also observed.

A complementary experiment was performed with L-[2,3-$^{13}C_2$]lysine in *F. nucleatum* (Table 12, Expt. 17). Since the L-[4,5-$^{13}C_2$]lysine experiment produced a ^{13}C-^{13}C-coupled butyrate, the butyrate produced from L-[2,3-$^{13}C_2$]lysine should not be a coupled unit provided either a racemase or the D-lysine pathway is absent (Table 7). Similar to the L-[4,5-$^{13}C_2$]lysine experiments, ^{13}C-labelled butyrate was isolated as the 4-bromophenacyl ester. The $^{13}C_2$ enrichment in butyrate was only 0.4%, significantly less than the 5.4% enrichment observed in the L-[4,5-$^{13}C_2$]lysine experiment (Table 12, Expt. 15) even though there was a higher initial level of $^{13}C_2$ enrichment in L-[2,3-$^{13}C_2$]lysine compared to L-[4,5-$^{13}C_2$]lysine. Hence, the results obtained from the L-[2,3-$^{13}C_2$]lysine experiment validate those from the L-[4,5-$^{13}C_2$]lysine experiment, and it can be suggested

that L-lysine in *F. nucleatum* is degraded via cleavage between C-2 and C-3 (Figure 6).

In *F. varium*, similar conclusions were obtained. Although, when L-[4,5-$^{13}C_2$]lysine was administered to *F. varium* (Table 12, Expt. 16), the $^{13}C_2$ enrichment found in butyrate was lower (0.9%) than the enrichment produced by *F. nucleatum* (5.4%). Due to the low enrichment observed, it was difficult to suggest at this stage whether L-lysine catabolism in *F. varium* proceeds via cleavage between C-2 and C-3. However, it must also be considered that the interconversion of butyrate with acetate in *F. varium* (Table 4, Expt. 2) is greater than that in *F. nucleatum* (Table 4, Expt. 1). The higher interconversion rate may explain the low $^{13}C_2$ enrichment due to the loss of doubly labelled butyrate in the interconversion process.

To provide a more conclusive result regarding the catabolism of L-lysine by *F. varium*, a complementary feeding experiment using L-[2,3-$^{13}C_2$]lysine was performed (Table 12, Expt. 18). Similar to the L-[2,3-$^{13}C_2$]lysine experiment in *F. nucleatum*, the $^{13}C_2$ enrichment in butyrate was only 0.4%. This level of enrichment is still less than half of the enrichment observed in the L-[4,5-$^{13}C_2$]lysine experiment (Table 12, Expt. 16). The results obtained from L-[2,3-$^{13}C_2$]lysine complement those obtained from L-[4,5-$^{13}C_2$]lysine, and it can be suggested that L-lysine in *F. varium* is also degraded via cleavage between C-2 and C-3 (Figure 6).

Furthermore, the L-[2,3-^{13}C$_2$]lysine experiments in both *F. nucleatum* and *F. varium* (Table 12, Expts. 17 and 18) provide another piece of evidence supporting cleavage between C-2 and C-3 that should not be overlooked. In the mixtures of singly ^{13}C-labelled butyrates, there is significantly more [1-^{13}C]- and [2-^{13}C]butyrate than [3-^{13}C]- and [4-^{13}C]butyrate. An interpretation of these results supporting cleavage between C-2 and C-3 (Figure 6) is presented in Figure 22.
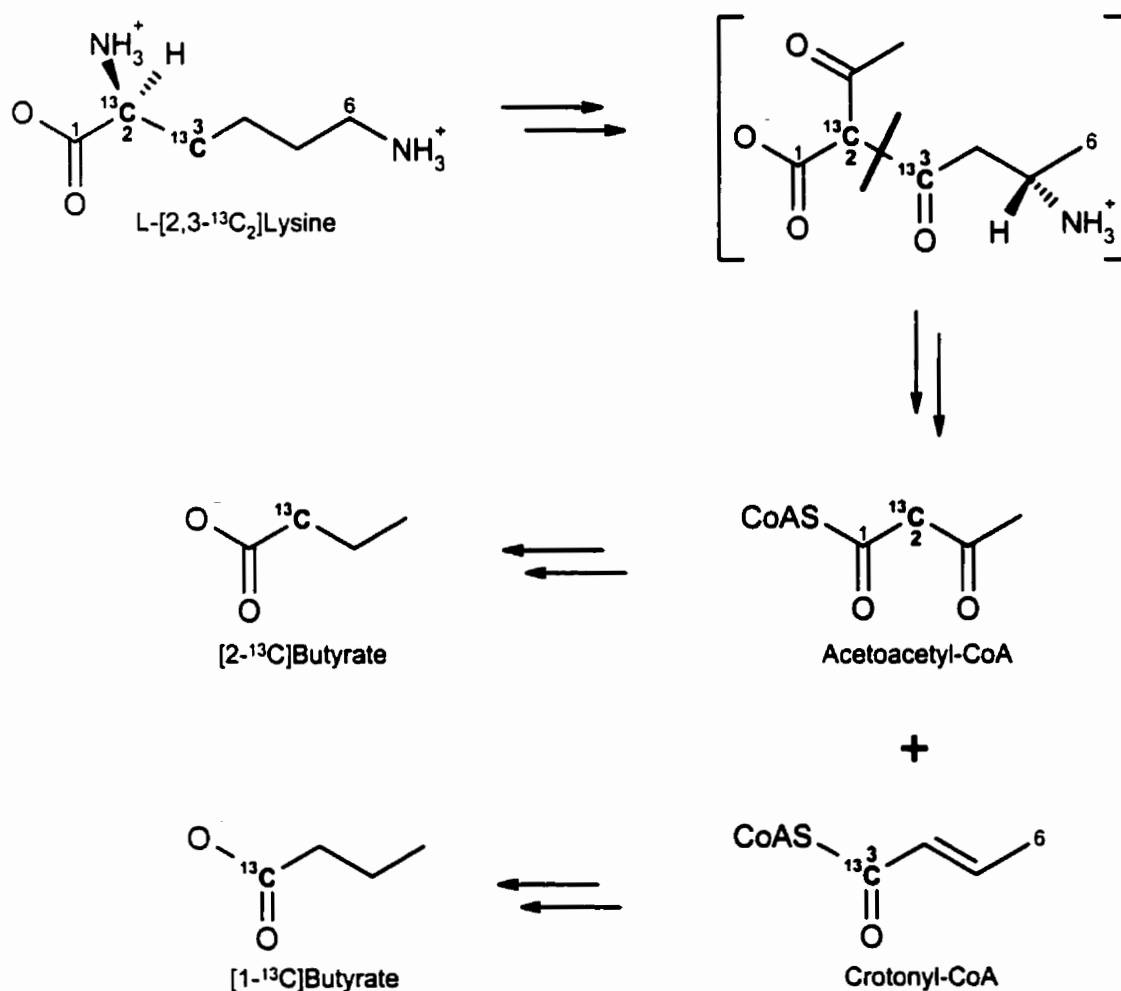
Figure 22. Degradation of L-[2,3-^{13}C$_2$]lysine via cleavage between C-2 and C-3 to yield [1-^{13}C]- and [2-^{13}C]butyrate.

The higher amounts of [1-^{13}C]- and [2-^{13}C]- compared to [3-^{13}C]- and [4-^{13}C]-labelled butyrate suggest that L-lysine cleavage occurs via the steps shown in Figure 22. The smaller quantities of [3-^{13}C]- and [4-^{13}C]butyrate are possibly due to the interconversion of the [1-^{13}C]- and [2-^{13}C]butyrate with acetate, causing label scrambling when butyrate is reformed.

It is also important to note that the catabolism of L-[2,3-^{13}C$_2$]lysine produces more [1-^{13}C]butyrate than [2-^{13}C]butyrate. [1-^{13}C]Butyrate is derived from crotonyl-CoA, while [2-^{13}C]butyrate arises from acetoacetyl-CoA (Figure 22). As shown in Figure 1, fewer metabolic steps are needed to convert crotonyl-CoA to butyrate, accounting for the higher incorpration of label into C-1 of butyrate. On the other hand, it is metabolically simpler for acetoacetyl-CoA to interconvert with acetate and cause scrambling of the ^{13}C-label. Furthermore, since the degradation of L-lysine via a C$_8$ intermediate is achieved by the addition of acetyl-CoA, acetyl-CoA must be regenerated by the cleavage of acetoacetyl-CoA into acetyl-CoA, which further encourages label scrambling.

As a package, the ^{13}C$_2$-labelled L-lysine experiments (Table 12) demonstrate that the degradation of L-lysine by *F. nucleatum* and *F. varium* occurs via a pathway similar to that found in the *Clostridium* species (Figure 6). Unambiguous isotopic evidence has revealed the presence an uncommon C$_8$ intermediate, found in the 3-keto-5-aminohexanoate pathway of L-lysine metabolism.

What remains to be studied, however, are the aspects of D-lysine catabolism and whether a lysine racemase is present in the two *Fusobacterium* species. Referring to Table 7, Case #3 and Case #4 have already been eliminated, leaving Case #1 and Case #2 to be distinguished by D-$[2,3-^{13}C_2]$- and D-$[4,5-^{13}C_2]$lysine experiments. Enantiomerically pure $^{13}C_2$-enriched D-lysine would have to be resynthesized.

In terms of L-lysine, both the results from the universally and $^{13}C_2$-labelled lysine experiments indicate that *F. nucleatum* and *F. varium* degrade lysine by similar pathways. This observation is rather striking, given the differences in the catabolism of glutamate and histidine observed between the two organisms. However, because the isotopic results indicate similar lysine pathways does not imply that the enzymatic steps are identical. What can be concluded, though, is that L-lysine is degraded to butyrate via C-2/C-3 cleavage, as found in the *Clostridium* species.

Chapter 5: Conclusions

The catabolism of the amino acids glutamate, histidine, and lysine by two *Fusobacterium* species were investigated in this study. Both isomers of the amino acids were catabolized, but the D-isomers were utilized slower than the corresponding L-amino acids. The lower rates observed may indicate the presence of amino acid racemases that convert the D-isomers to the L-isomers prior to degradation. Future studies to verify the presence of these racemases would be beneficial, as in general, racemases are not well characterized, especially amongst anaerobic bacteria.

In principle, butyrate can be formed from the three amino acids either directly from the amino acid as an intact four-carbon unit or from the combination of acetate derivatives. These two modes were investigated using isotopic labelling. In *F. nucleatum*, all three amino acids produced butyrate originating as an intact four-carbon unit, while in *F. varium*, this method of formation was observed only with lysine. The similarities observed in the catabolism of glutamate and histidine by both organisms support the theory that histidine is converted to glutamate prior to degradation. Histidine catabolism has not been explored in great detail in *Fusobacterium*, and further studies of its catabolism would be worthwhile.

Finally, the catabolism of L-lysine into butyrate was investigated. $^{13}C_2$-Labelled D- and L-lysine samples were analyzed for isotopic enrichment and

enantiomeric purity, and it was determined that only the L-lysine samples were sufficiently pure for use. The L-lysine backbone is cleaved between atoms C-2 and C-3 to form butyrate derived from atoms C-3 to C-6, supporting the 3,5-diaminohexanoate pathway of lysine catabolism. Future work should concentrate on investigating D-lysine catabolism and the enzymatic reactions associated with the catabolism of both lysine stereoisomers.

Chapter 6: Experimental

6.1 General Methods

All chemicals were purchased commercially and used without further purification unless otherwise indicated. Spectrophotometric measurements were performed in 1-cm quartz cuvettes on a Hewlett Packard 8452A diode array spectrophotometer. Except during inoculation, all manipulations of cells were performed in oxygen-reduced environments in an anaerobic glove bag that had been purged with nitrogen. PBS was made anaerobic by repeated cycles of evacuating and pressurizing with $H_2:CO_2:N_2$ (10:10:80 v/v) and consisted of 138 mM NaCl, 2.7 mM KCl, 5 mM sodium hydrogen phosphate, and 5 mM sodium dihydrogen phosphate; the pH of the solution was adjusted to 7.4 with 0.5 M NaOH. NMR spectra were collected on Bruker AC 250F (^1H at 250 MHz and ^{13}C at 62.9 MHz) and AMX 400 (^{13}C at 100.6 MHz) spectrometers. All FID data were processed in Bruker WinNMR. Chemical shifts were calibrated using $CDCl_3$ (δ = 77.0 ppm) or HOD (δ = 4.8 ppm) and are reported relative to tetramethylsilane. The HPLC system consisted of two Beckman 110B pumps, a Beckman 340 gradient mixer with a 210A injector, a Beckman 157 fluorescence detector with excitation (305-395 nm) and emission (420-650 nm) filters, and an HP 1050 UV detector. A Micromass VG Quattro mass spectrometer was used for the acquisition of mass spectra under electrospray ionization.

6.2 Growth of *F. nucleatum* and *F. varium*

F. nucleatum (ATCC 25586) and *F. varium* (NCTC 10560) were subcultured at weekly intervals and maintained at 37 °C on sheep-blood agar plates (Queen Elizabeth II Health Sciences Centre, Halifax, NS, Canada) in anaerobic jars (Oxoid, Unipath Inc., Nepean, ON, Canada) equipped with active palladium catalyst and filled with a $H_2:CO_2:N_2$ (10:10:80 v/v) atmosphere. Peptone medium containing (per litre) 0.8 g of L-cysteine hydrochloride and 5.0 g each of sodium chloride, D-glucose, trypticase peptone (BBL, Becton Dickinson and Co., Cockeysville, MD, USA), yeast extract (Difco Laboratories, Detroit, MI, USA), and proteose peptone (Difco Laboratories) was adjusted to pH 7.4 with 5 M NaOH and autoclaved. A loopful of *F. nucleatum* or *F. varium* cells grown on a sheep-blood agar plate for 48 h were transferred into peptone medium (10-20 mL) and incubated at 37°C in anaerobic jars; after 24-48 h, 10 mL of the culture was used to inoculate one litre of peptone medium. Cultures were harvested in late-exponential growth phase (OD_{660} = 1.0 after accounting for two-fold dilution; incubation in anaerobic jars at 37 °C for 20-24 h for *F. nucleatum* or 12-14 h for *F. varium*) by centrifugation (10 000 g, 10 min, 37 °C) in sealed O-ring centrifuge bottles. The pellet was resuspended and washed with anaerobic PBS solution (25 mL) and centrifuged, yielding 3-4 g of wet cell mass per litre of culture.

6.3 Determination of Amino Acid Utilization by HPLC and Identification of Acidic Metabolic End-Products by ^{1}H-NMR

Late-log-phase cells from 500 mL of liquid culture were divided into equal portions and each resuspended in PBS solution (25 mL). One portion was supplemented with an L-amino acid (10 mM), and the other portion with the D-isomer of the corresponding amino acid (10 mM). After flushing with three cycles of evacuating and pressurizing with $H_2:CO_2:N_2$ (10:10:80 v/v), the resuspensions were incubated at 37 °C with gentle agitation (100 rpm).

HPLC determination of amino acid utilization. At various times, samples (0.5 mL) were removed anaerobically with a syringe and centrifuged (15 400 *g*, 1 min). Supernatants were stored at –20 °C until ready for use. Supernatants (20 μL) diluted with water (1.98 mL) were derivatized using *o*-phthalaldehyde and mercaptoethanol, and the isoindole derivatives were separated on a Beckman ODS Ultrasphere column (5 μm, 45 × 4.6 mm). Gradients were formed between sodium acetate (pH 6.2):methanol:THF (900:95:5) and methanol.[19] The following gradients (min, % methanol) were used for the respective amino acids: lysine (0.0, 0; 0.5, 15; 3.0, 15; 3.3, 30; 4.3, 30; 4.5, 50; 6.3, 50; 7.0, 100; 7.5, 0), glutamate (0.0, 0; 0.5, 10; 1.5, 10; 2.0, 45; 3.0, 45; 4.0, 100; 4.5, 100; 5.0, 100), and histidine (0.0, 0; 0.5, 15; 2.0, 15; 3.0, 50; 3.8, 50; 4.8, 100; 5.0, 0). Residual amino acid concentrations (expressed as %) were calculated by comparing the peak area of the amino acid at various times to that measured initially; triplicate injections have demonstrated that the standard deviation is less than 2%.

Identification of acidic metabolic end-products by ¹H-NMR. Samples (10

mL) for ¹H-NMR analysis were centrifuged (10 000 g, 15 min, 4°C); the

supernatants were titrated to pH 10 with 5-M NaOH and evaporated to dryness in

vacuo. Portions (0.1 g) of the residues were dissolved in D_2O (1 mL) for the

acquisition of ¹H-NMR spectra. Samples were spiked with authentic compounds

(1-2 mg) to confirm the identity of the metabolic end-products acetate [δ (ppm):

1.9], butyrate [δ (ppm): 0.9 (t, J = 7.3 Hz, 3H), 1.5-1.6 (m, 2H), 2.2 (t, J = 7.3 Hz,

2H)], formate [δ (ppm): 8.6 (s)], and the residual substrates. The relative amounts

of the amino acid and the end-products were calculated using the integrated

areas of the NMR signals.

6.4   Determination of Substrate Utilization and Identification of Acidic Metabolic End-Products by ¹H-NMR

Feeding experiments involving substrates (Tables 2 and 3) other than

stereoisomers amino acids were performed similar to Section 6.3. Late-log-phase

cells from 250 mL of liquid culture were resuspended in PBS solution (25 mL)

supplemented with various substrates. After flushing with three cycles of

evacuating and pressurizing with $H_2:CO_2:N_2$ (10:10:80 v/v), the resuspensions

were incubated at 37 °C with gentle agitation (100 rpm) for 2.5 h. At the end of

the incubation period, resuspensions were as per Section 6.3 for NMR analysis.

6.5 Catabolism of ^{13}C-Labelled Substrates

Sodium [1,2-^{13}C$_2$]acetate (99% ^{13}C), sodium [1-^{13}C]butyrate (99% ^{13}C), L-[U-^{13}C$_5$]glutamate (97-98% ^{13}C), L-[U-^{13}C$_5$]histidine (97-98% ^{13}C), and L-[U-^{13}C$_6$]lysine (97-98% ^{13}C) were obtained from Cambridge Isotope Laboratories (Andover, MA, USA), and L-[1-^{13}C]-glutamate (99% ^{13}C) was acquired from C/D/N Isotopes Inc. (Vaudreuil, QC, Canada). Labelled compounds were diluted to the desired enrichment levels before use.

Late-log-phase cells from 500 mL of liquid culture were resuspended in PBS solution (50 mL) supplemented with substrates; details are provided in Tables 4, 5, and 6. The resuspensions were incubated in anaerobic jars at 37°C with gentle agitation (100 rpm). All resuspensions containing ^{13}C-labelled substrates were incubated for 2.5 h except for the following: L-lysine with *F. nucleatum*, 5.0 h; L-histidine with *F. varium*, 24 h; and L-histidine with *F. nucleatum*, 8.0 h. The resuspensions were centrifuged; the supernatants were titrated to pH 10 with NaOH and freeze-dried to yield a residue containing the sodium salts of the acidic end-products.

6.6 Determination of ^{13}C Enrichments in Acetate and Butyrate

Preparation and separation of 4-bromophenacyl acetate and butyrate. In the 10 mM sodium acetate and butyrate experiments, the residue was combined with 4-bromophenacyl bromide (0.40 g) and dicyclohexano-18-crown-6 (30 mg) and refluxed in acetonitrile (35 mL). For the 100 mM sodium acetate

experiments, the components were increased to 1.70 g, 130 mg, and 100 mL, respectively. The reaction mixture was refluxed and monitored by TLC (silica gel, dichloromethane) for the formation of 4-bromophenacyl acetate (R_f 0.4) and 4-bromophenacyl butyrate (R_f 0.7). When the relative intensities of the esters and excess 4-bromophenacyl bromide (R_f 0.8) became constant after 5-10 h, the reaction mixture was filtered through sintered glass and washed with acetonitrile (4 × 10 mL), and the filtrate was evaporated *in vacuo*. The oily residue was dissolved in a minimal amount (10-15 mL) of carbon tetrachloride and loaded onto a dry, flash chromatography column (15 g) prepared from silica gel (Aldrich, 70-230 mesh, 60 Å, previously dried for 1 h at 100 °C and cooled overnight in a desiccator). The column was eluted by stepwise gradients of dichloromethane:cyclohexane, ranging from 30 to 60% dichloromethane (v/v). Fractions (20 mL) were collected and analyzed by TLC; those visibly containing only the acetate or butyrate 4-bromophenacyl esters were pooled separately and evaporated *in vacuo*. Depending on the efficiency of the separation, 20-100 mg of each ester were obtained.

Isotopic analysis by NMR. The 4-bromophenacyl derivatives were dissolved in $CDCl_3$ (1 mL), and ^{13}C-NMR spectra were acquired at 62.9 MHz using standard Bruker acquisition parameters that included a 15.6 k spectral window, 32 k data points, and delay time (D1) of 2 s. Typically, 360-9600 scans were acquired, depending on the amount of sample available. FID data were processed with a line broadening of 3 Hz. Spectra for natural abundance

samples were acquired immediately following the acquisition of the corresponding ^{13}C-enriched spectra to minimize any variation in the acquisition conditions. The percent ^{13}C-enrichments were calculated from the heights of the acetate (20.6 and 170.4 ppm) and the butyrate signals (13.6, 18.4, 35.7, and 173.0 ppm) as described,[63] and a standard deviation of 0.1% in the enrichments was calculated from the peak heights of the natural abundance signals contributed by the derivatization reagent.

For the measurement of two- and three-bond ^{13}C-^{13}C coupling, ^{13}C-NMR spectra were acquired at 100.6 MHz using a 30.5 k spectral window, 128 k data points, and a delay time (D1) of 2 s. Typically, 250-18500 scans were acquired. FID data were processed with a line broadening of –0.75 Hz.

6.7 Analysis of [^{13}C$_2$]Lysine

The provided lysine samples[92] were analyzed for enantiomeric purity and isotopic enrichment.

6.7.1 Quantitative Enantiomeric Analysis of Lysine by FDA-HPLC

The enantiomeric analysis of lysine by HPLC was performed according to published procedures[93,94] with various modifications to accommodate differences in the equipment.

Preparation of FDA-derivatives for HPLC analysis. Lysine samples were dissolved in water (5.5 µmol per 1000 µL). FDA reagent was prepared by

dissolving 3.6 μmol FDA in 1000 μL acetonitrile:acetone (4:1). The derivatization

mixture was prepared by combining 8 μL of the lysine solution with 1.3 μL water,

14 μL acetonitrile, 4.7 μL triethylamine, and 40 μL FDA reagent. The molar ratio

of FDA to lysine was 2.8:1.0 to accommodate for the presence of two reactive

amino groups in lysine and also have excess FDA remaining. The reaction

mixture was placed into a reaction vial, capped, and incubated at 50 °C for 2 h.

After the incubation, the mixture was evaporated to dryness in a vacuum

desiccator, and the orange residue was dissolved in 250-500 μL

dimethylsulfoxide.

Analysis of FDA derivatives by HPLC. Diastereomeric FDA derivatives of

D- and L-lysine in the dimethylsulfoxide solution were separated on a CSC

Spherisorb ODS2 column (15 cm x 0.46 cm, 5 μm) at a flow rate of 2.50 mL/min

using a gradient established between triethylammonium phosphate (50 mM, pH

3.0) and acetonitrile:2-propanol (4:1 v/v). The following gradient (min, %

acetonitrile:2-propanol) was used for the analysis: 0.0, 0; 7.2, 20; 24.0, 36; 25.0,

100; 27.0, 100; 28.5, 0; 30.0, 0. Elution was monitored by UV absorption at 338

nm using a reference of 500 nm, with band widths of 10 nm and 80 nm,

respectively.

Calculation of response factors. Differences in the response of the

detector to the two diastereomers required a correction factor to be introduced. A

standard mixture D- and L-lysine was derivatized and injected in triplicate.

Response factors were calculated by comparing the average peak areas of the

two resolved D- and L-lysine derivatives, corrected for the known ratio of D- and L-lysine in the standard mixture. The response of the FDA derivative of D-lysine is typically 10% greater than that of the L-lysine derivative.

Determination of enantiomeric ratio in unknown lysine samples. Samples were prepared, derivatized, and injected in duplicate. The peak areas of the resolved diastereomers were corrected by the previously calculated response factor. The ratio of the corrected areas represented the ratio of D- and L-lysine.

6.7.2 MS Analysis of Lysine for $^{13}C_2$ Enrichment

Lysine samples (1 mg) were dissolved in water (1 mL), and 5 µL portions were injected into the mass spectrometer operating in cation electrospray mode at a cone voltage of 20 V and a scan range of m/z = 20-200. Natural abundance lysine samples were detected via an ion peak at m/z = 147, with no isotopic contribution to m/z = 149. Lysine samples containing $^{13}C_2$ enrichment produced signals at both m/z = 147 and m/z = 149. The % $^{13}C_2$ enrichment was calculated from the intensities of the m/z = 147 and m/z = 149 peaks; details are provided in Table 9.

6.7.3 Preparative-Scale Preparation, Separation, and Analysis of the FDA derivatives of D-[2,3-$^{13}C_2$]- and D-[4,5-$^{13}C_2$]Lysine

Due to the lack of enantiomeric purity and low $^{13}C_2$ enrichment of the two $^{13}C_2$-labelled D-lysine samples (Table 10), each enantiomer in both mixtures were

converted to diastereomers using FDA, separated by HPLC, and analyzed by MS in order to determine the exact $^{13}C_2$ enrichment of each enantiomer.

6.7.3.1 Preparation of the FDA derivatives

Lysine (1 mg) of approximately racemic mixture, either natural abundance or $^{13}C_2$-enriched, was dissolved in 400 µL water. FDA reagent, prepared by combining 1400 µL acetonitrile:acetone (4:1 v/v), 5.6 mg FDA, and 50 µL triethylamine, was added to the lysine solution. The mixture was placed in a capped reaction vial and incubated at 50 °C for 3 h. At the end of the incubation period, the mixture was dried in a vacuum desiccator and redissolved in 250 µL dimethylsulfoxide for subsequent separation by HPLC.

6.7.3.2 Separation of FDA derivatives of Lysine by HPLC

HPLC conditions. Diastereomeric derivatives were separated on a CSC Spherisorb ODS2 column (15 cm x 0.46 cm, 5 µm) at a flow rate of 2.50 mL/min on a gradient established between two solvents, A and B. Solvent A was prepared by adjusting 100 mM ammonium acetate to pH 3 with trifluoroacetic acid, while solvent B consisted of acetonitrile:2-propanol (4:1 v/v). The following gradient (min, % B) was used for the separation of the two diastereomers: 0.0, 0; 2.5, 20; 20.0, 36; 21.5, 100; 22.5, 100; 23.5, 0; 25.0, 0. Elution was monitored by UV absorption at 338 nm using a reference of 500 nm, with band widths of 10 nm and 80 nm, respectively.

Collection of separated derivatives. A portion (20 µL) of the dimethylsulfoxide solution was injected and monitored for derivative elution. The two peaks representing the two diastereomeric derivatives were collected from the tubing after they eluted from the column and through the UV detector. Approximately 2-3 mL were collected from each peak. Retention times were approximately 14 min and 17 min for the derivatives of L- and D-lysine, respectively. Twelve injections were required to process the 250 µL of solution; after the last injection, the sample vial was washed three times with 20 µL dimethylsulfoxide each, injecting the washing after each wash. Collected peaks corresponding to each diastereomer were pooled separately and evaporated *in vacuo* until approximately 10 mL of liquid remained, producing a cloudy yellow solution.

Removal of the buffer system from the separated derivatives. Each solution of separated derivatives was diluted with 25 mL water:acetonitrile (4:1 v/v) in a flask, after which most of the cloudiness disappeared. A few yellow flakes remained in suspension. The solution was adjusted to pH 1.5-2.0 with trifluoroacetic acid and loaded under vacuum onto a Fisher C_{18} Prep-Sep column that had been previously conditioned with methanol and rinsed with water. At a low pH, the derivative is presumably in its neutral form, enhancing adherence to the hydrophobic column. The flask was rinsed with 10 mL water:acetonitrile (4:1 v/v), and its contents adjusted to pH 1.5-2.0 with trifluoroacetic acid and then also loaded onto the column. The column was washed under vacuum with two 5 mL

portions of water, discarding the washings. The yellow residue, which remained on the column, was eluted with 10 mL triethylamine:acetonitrile:water (2:49:29) and collected. The high pH presumably ionizes the derivative to promote elution and increase solubility, and it also dissolved the yellow flakes remaining at the surface of the column frit. The sample was evaporated to dryness in a vacuum desiccator, yielding a brilliant yellow flaky residue containing presumably one pure diastereomer and a minimal amount of the ammonium acetate-fluoroacetate buffer system.

6.7.3.3 Analysis of the Separated and Cleaned FDA derivatives by MS

The sold residues were dissolved in 60 µL triethylamine:acetonitrile:water (2:3:3); the triethylamine improves solubility and enhances sample ionization in the mass spectrometer. After diluting the samples with 200 µL acetonitrile:water (1:1 v/v), the solvent system used with the mass spectrometer, approximately 5 µL were injected. Conditions for the instrument, operating in anion electrospray mode, included a cone voltage of 10 V and a scan range of m/z = 550-700. Ion peaks were observed at m/z = 649 and m/z = 651, corresponding to unenriched and $^{13}C_2$-enriched species, respectively. Details and calculations of $^{13}C_2$ enrichment are provided in Table 11.

6.7.3.4 Assessment of the Diastereomeric Purity of the Separated FDA Derivatives

Ideally, the derivatives used for MS analysis (Section 6.7.3.3) should contain only one diastereomer, i.e. the FDA derivative of either L- or D-lysine. The diastereomeric purity depended on the efficiency of the HPLC separation (Section 6.7.3.2), which theoretically should have been very effective. Nonetheless, the samples used for MS analysis, representative of the pooled HPLC separations, were re-analyzed by HPLC.

From each of the samples analyzed by MS, approximately 0.5 μL were removed, transferred to a test tube, and dried in a vacuum desiccator. Dimethylsulfoxide (25 μL) was added to dissolve the residue, and 20 μL of the solution was injected into the HPLC instrument. Conditions were identical with those used in the original separation (Section 6.7.3.2). The diastereomeric purity was estimated from the peak areas to be greater than 98% or 99%, indicating that the original preparative-scale separation was efficient.

6.8 Dilution of ^{13}C Enrichments in L-[2,3-^{13}C$_2$]- and L-[4,5-^{13}C$_2$]Lysine

Preparation of dihydrochloride salts. Once the enantiomeric purities of the provided ^{13}C$_2$-labelled lysine samples[92] were determined, the two L-lysine free base samples were converted to their respective dihydrochloride salts; the D-lysine samples were not processed due to their near-racemic purity. The L-lysine samples were dissolved in water and titrated with HCl to pH 2.2, the pKa$_2$ of

lysine. The total volume of HCl required to reach pH 2.2 is representative of 1.5 equivalents. An additional 0.7 equivalents were added, providing a molar ratio of HCl:lysine of 2.2:1 to include some excess HCl. The flask contents were evaporated to dryness *in vacuo* to remove excess HCl, and the residue was dissolved in H_2O and freeze dried. Approximately 130-160 mg of lysine dihydrochloride were recovered.

Isotopic dilution and analysis of the dihydrochloride salts. Each of the labelled lysine dihydrochloride samples was combined with unenriched L-lysine dihydrochloride to yield a total of 0.50 mmol L-lysine (50 mL of a 10 mM solution at 10-15% $^{13}C_2$ enrichment required for each feeding experiment). Typically, 25 mg of the labelled material was combined with 80 mg of unlabelled lysine. To determine the exact $^{13}C_2$ enrichment, the isotopically diluted samples above were each dissolved in D_2O (2 mL) and thoroughly mixed. Portions (1 mL) of each solution (1 mL) were removed for ^{13}C-NMR analysis at 62.9 MHz. A natural abundance sample of lysine dihydrochloride (50 mg in 1 mL D_2O) was also analyzed. The labelled samples displayed two sets of doublets corresponding to atoms C-2 and C-3 or C-4 and C-5 of lysine. Similar to the analysis of ^{13}C-enrichments in 4-bromophenacyl esters of acetate or butyrate, the unlabelled atoms of the lysine moiety were used for the normalization and calculation of ^{13}C-enrichments. Typical $^{13}C_2$-enrichments in the diluted samples were approximately 13-15%.

6.9 L-[2,3-$^{13}C_2$]- and L-[4,5-$^{13}C_2$]Lysine Feeding Experiments

The $^{13}C_2$-enriched lysine solutions (Section 6.9) were freeze dried to remove the D_2O and redissolved in 50 mL anaerobic PBS containing 10 mM sodium acetate.

Feeding experiments were performed as per Section 6.5. Briefly, late-log-phase cells from 500 mL of liquid culture were resuspended with the lysine and acetate PBS solutions prepared above. The resuspensions were incubated in anaerobic jars at 37°C and 100 rpm for 5.0 h (*F. nucleatum*) or 3.0 h (*F. varium*). The resuspensions were centrifuged, and the supernatants were titrated to pH 10 with NaOH and freeze-dried. The residue was derivatized as per Section 6.6 for analysis of isotopic enrichments.

References

1. Levett, P. N. *Anaerobic Bacteria, A Functional Biology*; Open University Press: Philadelphia, 1990.

2. Zeikus, J. G. *Ann. Rev. Microbiol.* **1980**, *34*, 423-64.

3. Jackins, H. C.; Barker, H. A. *J. Bacteriol.* **1951**, *16*, 101-114.

4. Loesche, W. J.; Gibbons R. J. *Archs. Oral. Biol.* **1968**, *13*, 191-201.

5. Rogers, A. H.; Zilm, P. S.; Gully, N. J.; Pfenning, A. L.; Marsh, P. D. *Oral Microbiol. Immunol.* **1991**, *6*, 250-255.

6. Robrish, S. A.; Oliver, C.; Thompson, J. *J Bacteriol.* **1987**, *169*, 3891-3897.

7. Gharbia, S. E.; Shah, H. N. *Curr. Microbiol.* **1988**, *17*, 229-234.

8. McInerney, M. J.; Anerobic hydrolysis and fermentation of fats and proteins; In *Biology of Anaerobic Microorganisms*; John Wiley and Sons: New York, 1988; pp 373-445.

9. Bugg, T. D. H.; Walsh, C. T. *Nat. Prod. Rep.* **1992**, *9*, 199-215.

10. Chu, D. T. W.; Plattner, J. J.; Katz, L. *J. Med. Chem.* **1996**, *39*, 3853-3874.

11. Henry, C. M. *Chem. Eng. News* **2000**, March 6, 41-58.

12. Satyanarayana, S.; White, R. L. *Dal. Med. Journal* **1999**, *27*, 45-52.

13. Bolstad, A. I.; Jensen, H. B.; Bakken, V. *Clin. Microbiol. Rev.* **1996**, *9*, 55-71.

14. Bakken, V.; Hogh, B. T.; Jensen, H. B. *Scand. J. Dent. Res.* **1989**, *97*, 43-53.

15. Gharbia, S. E.; Shah, H. N. *Curr. Microbiol.* **1989**, *18*, 189-193.

16. Zink, J. L.; Socransky, S. S. *Oral. Microbiol. Immunol.* **1990**, *5*, 172-174.

17. Gharbia, S. E.; Shah, H. N.; Welch, S. G. *Curr. Microbiol.* **1989**, *19*, 231-235.

18. Gharbia, S. E.; Shah, H. N.; *Oral. Microbiol. Immunol.* **1991**, *6*, 264-269.

19. Ramezani, M.; MacIntosh, S. E.; White, R. L. *Amino Acids* **1999**, *17*, 185-193.

20. Barker, H. A.; Bacterial Fermentations; In *CIBA Lectures in Microbiology and Biochemistry*; John Wiley and Sons, Inc: New York, **1956**.

21. Smith, G. M.; Kim, B. W.; Franke, A. A.; Roberts, J. D. *J. Biol. Chem.* **1985**, *260*, 13509-13512.

22. Wolff, R. A.; Urben, G. W.; O'Herrin, S. M.; Kenearly, W. R. *Appl. Environ. Microbiol.* **1993**, 59, 1876-1882.

23. Barker, H.A.; Kahn, J. M.; Hendrick, L. *J. Bacteriol.* **1982**, *152*, 201-207.

24. Wohlfarth, G.; Buckel, W. *Arch. Microbiol.* **1985**, *142*, 128-135.

25. Bennett, G. N.; Rudolph, F. B. *FEMS Microbiol. Rev.* **1995**, *17*, 241-249.

26. Ramezani, M. *PhD thesis*; Dalhousie University, **1996**.

27. Buckel, W.; Semmler, R. *Eur. J. Biochem.* **1983**, *136*, 427-434.

28. Barker, H. A.; Fermentation of Nitrogenous Compounds; In *The Bacteria*; Academic Press: New York, **1961**; pp 151-207.

29. Wacshman, J. T.; Barker, H. A. *J. Biol. Chem.* **1955**, *217*, 695-702.

30. Barker, H. A.; Smith, R. D.; Wawaszkiewicz, E. J.; Lee, M. N.; Wilson, R. M. *Arch. Biochem. Biophys.* **1958**, *78*, 468-476.

31. Barker, H. A.; Weissbach, H.; Smyth, R. D. *Proc. Natl. Acad. Sci.* **1958**, *44*, 1093-1097.

32. Suzuki, F.; Barker, H. A. *J. Biol. Chem.* **1966**, *241*, 878-888.

33. Holloway, D. E.; Marsh, E. N. G. *FEBS Lett.* **1993**, *317*, 44-48.

34. Holloway, D. E.; Marsh, E. N. G. *J. Biol. Chem.* **1994**, *269*, 20425-20430.

35. Brecht, M.; Kellermann, J.; Plucktham, A. *FEBS Lett.* **1993**, *319*, 84-89.

36. Leutbecher, U.; Bocher, R.; Linder, D.; Buckel, W. *Eur. J. Biochem.* **1992**, *205*, 759-765.

37. Zelder, O.; Beatrix, B.; Buckel, W. *FEMS Micriobiol. Lett.* **1994**, *118*, 15-22.

38. Botting, N. P.; Akhtar, M.; Cohen, M. A.; Gani, D. *Biochemistry* **1988**, *27*, 2953-2955.

39. Botting, N. P.; Cohen, M. A.; Akhtar, M.; Gani, D. *Biochemistry* **1988**, *27*, 2956-2959.

40. Botting, N. P.; Gani, D. *Biochemistry* **1992**, *31*, 1509-1520.

41. Gani, D.; Archer, C. H.; Botting, N. P.; Pollard, J. R. *Bioorg. Med. Chem.* **1999**, *7*, 977-990.

42. Pollard, J. R.; Richardson, S.; Akhtar, M.; Lasry, P.; Neal, T.; Botting, N. P.; Gani, D. *Bioorg. Med. Chem.* **1999**, *7*, 949-975.

43. Goda, S. K.; Minton, N. P.; Botting, N. P.; Gani, D. *Biochemistry* **1992**, *31*, 10747-10756.

44. Wang, C. C.; Barker, H. A. *J. Biol. Chem.* **1969**, *244*, 2516-2526.

45. Blair, A. H.; Barker, H. A. *J. Biol. Chem.* **1966**, *241*, 400-408.

46. Wang, C. C.; Barker, H. A. *Meth. Enzymol.* **1969**, *13*, 331-344.

47. Barker, H. A. *Meth. Enzymol.* **1969**, *13*, 344-346.

48. Buckel, W.; Bobi, A. *Eur. J. Biochem.* **1976**, *64*, 255-262.

49. Bearne, S. L.; White, R. L.; MacDonnell, J.; Grønlund, J.; Bahrami, S. Unpublished experiments.

50. Buckel, W.; Barker, H. A. *J. Bacteriol.* **1974**, *117*, 1248-1260.

51. Johnson, W. M.; Westlake, D. W. S. *Bacteriol. Proc.* **1970**, *P196*, 153.

52. Kew, O. M.; Woolfolk, C. A. *Biochem. Biophys. Res. Comm.* **1970**, *39*, 1129-1133.

53. Lerud, R. F.; Whiteley, H. R. *Bacteriol. Proc.* **1970**, *P197*, 153.

54. Lerud, R. F.; Whiteley, H. R. *J. Bacteriol.* **1971**, *106*, 571-577.

55. Johnson, W. M.; Westlake, D. W. S. *Can. J. Microbiol.* **1969**, *47*, 1101-1107.

56. Buckel, W. *Eur. J. Biochem.* **1980**, 106, 439-447.

57. Schweiger, G.; Buckel, W. *Arch. Microbiol.* **1984**, *137*, 302-307.

58. Klees, A.; Linder, D.; Buckel, W. *Arch. Microbiol.* **1992**, *158*, 294-301.

59. Buckel, W. *Eur. J. Biochem.* **1986**, 156, 259-263.

60. Whiteley, H. R. *J. Bacteriol.* **1957**, *74*, 324-330.

61. Horler, D. F.; Westlake, D. W. S.; McConnell, W. B. *Can. J. Microbiol.* **1966**, *12*, 47-52.

62. Gharbia, S. E.; Shah, H. N. *J. Gen. Micriobiol.* **1991**, *137*, 1201-1206.

63. White, R. L.; Ramezani, M.; Gharbia, S. E.; Seth, R.; Doherty-Kirby, A. L.; Shah, H. N. *Biotechnol. Appl. Biochem.* **1995**, *22*, 385-396.

64. Beatrix, B.; Bendrat, K.; Rospert, S.; Buckel, W. *Arch. Microbiol.* **1990**, *154*, 362-369.

65. Bendrat, K.; Buckel, W. *Eur. J. Biochem.* **1993**, *211*, 697-702.

66. De Braekeleer, M. *Hum. Hered.* **1991**, *41*, 141-146.

67. Taylor, R. G.; Lambert, M. A.; Sexsmith, E.; Sadler, S. J.; Ray, P. N.; Mahuran, D. J.; McInnes, R. R. *J. Biol. Chem.* **1990**, *265*, 18192-18199.

68. Schwede, T. F.; Retey, J.; Schulz, G. E. *Biochemistry* **1999**, *38*, 5355-5361.

69. Retey, J. *Arch. Biochem. Biophys.* **1994**, *314*, 1-16.

70. Consevage, M. W.; Porter, R. D.; Phillips, A. T. *J. Bacteriol.* **1985**, *162*,138-146.

71. Beaudet, R.; Mackenzie, R. *Biochem. Biophys. Acta* **1975**, *410*, 252-261.

72. Stadtman, T. C. *Adv. Enzymol.* **1973**, *38*, 413-448.

73. Stadtman, T. C. *J. Bacteriol.* **1954**, *67*, 314.

74. Stadtman, T. C.; White, F. H. Jr. *J. Bacteriol.* **1954**, *67*, 651.

75. Yorifuji, T.; Jeng, I. M.; Barker, H. A. *J. Biol. Chem.* **1977**, *252*, 20-31.

76. Chirpich, T. P.; Zappia, V.; Costilow, R. N.; Barker, H. A. *J. Biol. Chem.* **1970**, *245*, 1778.

77. Zappia, V.; Barker, H. A. *Biochem. Biophys. Acta* **1970**, *125*, 226.

78. Ruzicka, F. J.; Lieder, K. W.; Frey, P. A. *J. Bacteriol.* **2000**, *182*, 469-476.

79. Stadtman, T. C.; Renz, P. *Arch. Biochem. Biophys.* **1970**, *125*, 226.

80. Kunz, F.; Retey, J.; Argoni, D.; Tsai, L.; Stadtman, T. C. *Helvetica Chim. Acta* **1978**, *61*, 1139.

81. Baker, J. J.; van der Drift, C.; Stadtman, T. C. *Biochemistry* **1973**, *12*, 1054.

82. Baker, J. J.; van der Drift, C.; Stadtman, T. C. *Fed. Proc.* **1972**, *31*, 494.

83. Rimermann, E. A.; Barker, H. A. *J. Biol. Chem.* **1968**, *243*, 6151.

84. Baker, J. J.; Barker, H. A. *J. Biol. Chem.* **1972**, *247*, 7724.

85. Yorifuji, T.; Jeng, I. M.; Barker, H. A. *J. Biol. Chem.* **1974**, *249*, 6578-6584.

86. Barker, H. A.; Jeng, I. M.; Neff, N.; Robertson, J. M.; Tam, F. K.; Hosaka, S. *J. Biol. Chem.* **1978**, *253*, 1219-1225.

87. Jeng, I. M.; Barker, H. A. *J. Biol. Chem.* **1974**, *249*, 6578-6584.

88. Morley, C. G. D.; Stadtman, T. C. *Biochemistry.* **1970**, *9*, 4890.

89. Morley, C. G. D.; Stadtman, T. C. *Biochemistry.* **1972**, *11*, 600.

90. Cao, X.; Kolonay, J. Jr.; Saxton, K. A.; Hartline, R. A. *Plasmid* **1993**, *30*, 83-89.

91. Fang, A.; Keables, P.; Demain, A. L. *Appl. Microbiol. Biotechnol.* **1996**, *44*, 705-709.

92. Witherell, R. D. *MSc thesis*; Dalhousie University, **1999**.

93. Marfey, P. *Carlsberg Res. Commun.* **1984**, *49*, 591-596.

94. Scaloni, A.; Simmaco, M.; Bossa, F. *Amino Acids* **1995**, *8*, 305-313.